and anti-HSP90 from Enzo Life Sciences Inc. (Farmingdale, NY, USA). Rabbit anti-human SOD1 antibody was raised against a recombinant human SOD1 peptide (24–36) and purified with protein A [40].

Immunoblotting

Tissues were homogenized in TNE lysis buffer [50 mM Tris–HCl (pH 7.4), 150 mM NaCl, 1 mM ethylenediaminetetraacetic acid (EDTA), 1% Triton-X 100, protease inhibitor cocktail (Roche, Basel, Switzerland)] with Dounce homogenizer. The lysates were centrifuged at 15,000 × g for 10 min at 4°C and the supernatants were collected. For the analyses of insoluble SOD1, the pellets were re-solubilized in the equivalent volume of TNE lysis buffer supplemented with 2% SDS and benzonase (Roche). After minutes of incubation at room temperature, the lysates were sonicated and centrifuged at 15,000 × g for 10 min. The supernatants were collected as insoluble fractions. All the protein content was measured by micro BCA assay kit (Thermo Fisher Scientific Inc., Waltham, MA, USA) and equal amounts of total proteins were analyzed by immunoblotting. Densitometric analysis was performed after the chemiluminescence detection by using an image analyzer LAS-4000mini (Fuji film, Tokyo, Japan) with the equipped software.

Immunoprecipitation

For the detection of HSF1 deacetylation, we slightly modified the previously reported procedure [14]. In brief, lumbar spinal cords were homogenized in radioimmunoprecipitation (RIPA) buffer [50 mM Tris–HCl (pH 8.0), 150 mM NaCl, 1% NP-40, 0.5% sodium deoxycholate, 0.1% SDS] supplemented with 1 mM EDTA, 2 mM nicotinamide and 1 mM trichostatin A (all from Sigma) with Dounce homogenizer. The lysates were centrifuged at 15,000 × g for 10 min at 4°C. Anti-HSF1 antibody (1:100) was added to the supernatant and incubated for over-night at 4°C with gentle agitation. Protein G sepharose (GE Healthcare, Waukesha, WI, USA; 15 μl each) was added and incubated for further 1.5 h. The beads were washed four times with phosphate buffered saline. The proteins were eluted with 2 × SDS loading buffer and heating at 95°C for 3 min. Deacetylated and total HSF1 were detected on the same polyvinylidene difluoride membrane with Restore western blot stripping buffer (Thermo).

Additional file

Additional file 1: Additional experimental procedures and figures.

Abbreviations

ALS: amyotrophic lateral sclerosis; CNS: central nervous system; SOD1: Cu/Zn-superoxide dismutase; EGFP: enhanced green fluorescent protein; HSF1: heat shock factor 1; HSP: heat shock protein; HSP70i: inducible heat shock protein 70; SD: standard deviation; SEM: standard error of the mean; $SOD1^{G93A}$-H: $SOD1^{G93A}$ high expression line; $SOD1^{G93A}$-L: $SOD1^{G93A}$ low expression line; SDS: sodium dodecyl sulfate.

Competing interests

The authors declare that they have no competing interests.

Authors' contributions

SW, SN, and NA-I conducted the biochemical, histological, behavioral analyses with supports from OK, FE, HM, and RT, under the supervision of KY and MK. KT and TM supervised the behavioral tests. MK and KY designed this study. SW, MK and KY wrote the manuscript. All authors read and approved the manuscript.

Acknowledgements

We thank D. Borchelt (University of Florida) for *Mo-Prp* DNA, S. Imai (Washington University) for mouse Sirt1 cDNA, A. Cvekl (Albert Einstein College of Medicine) for mouse αA-crystallin promoter DNA, and A. Tanigaki, R. Hikawa, C. Oshima, and H. Tsuiji for technical help in the establishment and/or analysis of the PrP-Sirt1 transgenic lines. This work was supported in part by CREST (Creation of a novel technology for prevention, diagnosis, and therapy for psychiatric and neurological disorders) from JST, Grant-in-Aid for Scientific Research on Innovative Areas (Foundation of Synapse Neurocircuit Pathology) (to MK and KY), Comprehensive Brain Science Network, and Grants-in-Aid for Scientific Research 23111006 (to KY), 22700404 (to SW) from the Ministry for Education, Culture, Sports and Science and Technology, Japan, and Grants-in-Aid from the Research Committee of CNS Degenerative Diseases, the Ministry of Health, Labor and Welfare of Japan, and Naito Foundation.

Author details

[1]Department of Neuroscience and Pathobiology, Research Institute of Environmental Medicine, Nagoya University, Furo-cho, Chikus, Nagoya 464-8601, Japan. [2]Department of Molecular Biology, Division of Biological Sciences, Nagoya University Graduate School of Science, Furo-cho, Chikusa, Nagoya 464-8602, Japan. [3]Laboratory for Motor Neuron Disease, RIKEN Brain Science Institute, Wako, Saitama, Japan. [4]Department of Pharmacology, Faculty of Pharmacy, Keio University, Tokyo, Japan. [5]Center for Genetic Analysis of Behavior, National Institute for Physiological Sciences, Okazaki, Japan. [6]Genetic Engineering and Functional Genomics Group, Frontier Technology Center, Kyoto University Graduate School of Medicine, Kyoto, Japan. [7]Division of Systems Medical Science, Institute for Comprehensive Medical Science, Fujita Health University, Toyoake, Japan. [8]Department of Neurology, Kyoto University Graduate School of Medicine, Kyoto, Japan. [9]CREST (Core Research for Evolutionary Science and Technology), JST (Japan Science and Technology Agency), Kawaguchi, Japan.

Received: 2 July 2014 Accepted: 14 August 2014
Published: 29 August 2014

References

1. Chiti F, Dobson CM: **Protein misfolding, functional amyloid, and human disease.** *Annu Rev Biochem* 2006, **75**:333–366.
2. Cleveland DW, Rothstein JD: **From Charcot to Lou Gehrig: deciphering selective motor neuron death in ALS.** *Nat Rev Neurosci* 2001, **2**:806–819.
3. Ferraiuolo L, Kirby J, Grierson AJ, Sendtner M, Shaw PJ: **Molecular pathways of motor neuron injury in amyotrophic lateral sclerosis.** *Nat Rev Neurol* 2011, **7**:616–630.
4. Valentine JS, Hart PJ: **Misfolded CuZnSOD and amyotrophic lateral sclerosis.** *Proc Natl Acad Sci U S A* 2003, **100**:3617–3622.
5. Gruzman A, Wood WL, Alpert E, Prasad MD, Miller RG, Rothstein JD, Bowser R, Hamilton R, Wood TD, Cleveland DW, Lingappa VR, Liu J: **Common molecular signature in SOD1 for both sporadic and familial amyotrophic lateral sclerosis.** *Proc Natl Acad Sci U S A* 2007, **104**:12524–12529.
6. Guareschi S, Cova E, Cereda C, Ceroni M, Donetti E, Bosco DA, Trotti D, Pasinelli P: **An over-oxidized form of superoxide dismutase found in sporadic amyotrophic lateral sclerosis with bulbar onset shares a toxic mechanism with mutant SOD1.** *Proc Natl Acad Sci U S A* 2012, **109**:5074–5079.
7. Shinder GA, Lacourse MC, Minotti S, Durham HD: **Mutant Cu/Zn-superoxide dismutase proteins have altered solubility and interact with heat shock/stress proteins in models of amyotrophic lateral sclerosis.** *J Biol Chem* 2001, **276**:12791–12796.
8. Koyama S, Arawaka S, Chang-Hong R, Wada M, Kawanami T, Kurita K, Kato M, Nagai M, Aoki M, Itoyama Y, Sobue G, Chan PH, Kato T: **Alteration of**

familial ALS-linked mutant SOD1 solubility with disease progression: its modulation by the proteasome and Hsp70. *Biochem Biophys Res Commun* 2006, **343**:719–730.
9. Yamashita H, Kawamata J, Okawa K, Kanki R, Nakamizo T, Hatayama T, Yamanaka K, Takahashi R, Shimohama S: **Heat-shock protein 105 interacts with and suppresses aggregation of mutant Cu/Zn superoxide dismutase: clues to a possible strategy for treating ALS.** *J Neurochem* 2007, **102**:1497–1505.
10. Bruening W, Roy J, Giasson B, Figlewicz DA, Mushynski WE, Durham HD: **Up-regulation of protein chaperones preserves viability of cells expressing toxic Cu/Zn-superoxide dismutase mutants associated with amyotrophic lateral sclerosis.** *J Neurochem* 1999, **72**:693–699.
11. Aridon P, Geraci F, Turturici G, D'Amelio M, Savettieri G, Sconzo G: **Protective role of heat shock proteins in Parkinson's disease.** *Neurodegener Dis* 2011, **8**:155–168.
12. Hoshino T, Murao N, Namba T, Takehara M, Adachi H, Katsuno M, Sobue G, Matsushima T, Suzuki T, Mizushima T: **Suppression of Alzheimer's disease-related phenotypes by expression of heat shock protein 70 in mice.** *J Neurosci* 2011, **31**:5225–5234.
13. Neef DW, Jaeger AM, Thiele DJ: **Heat shock transcription factor 1 as a therapeutic target in neurodegenerative diseases.** *Nat Rev Drug Discov* 2011, **10**:930–944.
14. Westerheide SD, Anckar J, Stevens SM Jr, Sistonen L, Morimoto RI: **Stress-inducible regulation of heat shock factor 1 by the deacetylase SIRT1.** *Science* 2009, **323**:1063–1066.
15. Han S, Choi JR, Soon Shin K, Kang SJ: **Resveratrol upregulated heat shock proteins and extended the survival of G93A-SOD1 mice.** *Brain Res* 2012, **1483**:112–117.
16. Mancuso R, Del Valle J, Modol L, Martinez A, Granado-Serrano AB, Ramirez-Nunez O, Pallas M, Portero-Otin M, Osta R, Navarro X: **Resveratrol improves motoneuron function and extends survival in SOD1 ALS Mice.** *Neurotherapeutics* 2014, **13**:419–432.
17. Boillee S, Yamanaka K, Lobsiger CS, Copeland NG, Jenkins NA, Kassiotis G, Kollias G, Cleveland DW: **Onset and progression in inherited ALS determined by motor neurons and microglia.** *Science* 2006, **312**:1389–1392.
18. Gurney ME, Pu H, Chiu AY, Dal Canto MC, Polchow CY, Alexander DD, Caliendo J, Hentati A, Kwon YW, Deng HX, Chen W, Zhai P, Sufit RL, Siddique T: **Motor neuron degeneration in mice that express a human Cu, Zn superoxide dismutase mutation.** *Science* 1994, **264**:1772–1775.
19. Urushitani M, Kurisu J, Tsukita K, Takahashi R: **Proteasomal inhibition by misfolded mutant superoxide dismutase 1 induces selective motor neuron death in familial amyotrophic lateral sclerosis.** *J Neurochem* 2002, **83**:1030–1042.
20. Kakefuda K, Fujita Y, Oyagi A, Hyakkoku K, Kojima T, Umemura K, Tsuruma K, Shimazawa M, Ito M, Nozawa Y, Hara H: **Sirtuin 1 overexpression mice show a reference memory deficit, but not neuroprotection.** *Biochem Biophys Res Commun* 2009, **387**:784–788.
21. Wu D, Qiu Y, Gao X, Yuan XB, Zhai Q: **Overexpression of SIRT1 in mouse forebrain impairs lipid/glucose metabolism and motor function.** *PLoS One* 2011, **6**:e21759.
22. Hattori Y, Okamoto Y, Maki T, Yamamoto Y, Oishi N, Yamahara K, Nagatsuka K, Takahashi R, Kalaria RN, Fukuyama H, Kinoshita M, Ihara M: **SIRT1 counters cerebral hypoperfusion injury by deacetylating eNOS.** *Stroke* 2014, in press.
23. Jiang M, Wang J, Fu J, Du L, Jeong H, West T, Xiang L, Peng Q, Hou Z, Cai H, Seredenina T, Arbez N, Zhu S, Sommers K, Qian J, Zhang J, Mori S, Yang XW, Tamashiro KL, Aja S, Moran TH, Luthi-Carter R, Martin B, Maudsley S, Mattson MP, Cichewicz RH, Ross CA, Holtzman DM, Krainc D, Duan W: **Neuroprotective role of Sirt1 in mammalian models of Huntington's disease through activation of multiple Sirt1 targets.** *Nat Med* 2012, **18**:153–158.
24. Jeong H, Cohen DE, Cui L, Supinski A, Savas JN, Mazzulli JR, Yates JR 3rd, Bordone L, Guarente L, Krainc D: **Sirt1 mediates neuroprotection from mutant huntingtin by activation of the TORC1 and CREB transcriptional pathway.** *Nat Med* 2012, **18**:159–165.
25. Donmez G, Arun A, Chung CY, McLean PJ, Lindquist S, Guarente L: **SIRT1 protects against alpha-synuclein aggregation by activating molecular chaperones.** *J Neurosci* 2012, **32**:124–132.
26. Donmez G, Wang D, Cohen DE, Guarente L: **SIRT1 suppresses beta-amyloid production by activating the alpha-secretase gene ADAM10.** *Cell* 2010, **142**:320–332.
27. Qin W, Yang T, Ho L, Zhao Z, Wang J, Chen L, Zhao W, Thiyagarajan M, MacGrogan D, Rodgers JT, Puigserver P, Sadoshima J, Deng H, Pedrini S, Gandy S, Sauve AA, Pasinetti GM: **Neuronal SIRT1 activation as a novel mechanism underlying the prevention of Alzheimer disease amyloid neuropathology by calorie restriction.** *J Biol Chem* 2006, **281**:21745–21754.
28. Montie HL, Pestell RG, Merry DE: **SIRT1 modulates aggregation and toxicity through deacetylation of the androgen receptor in cell models of SBMA.** *J Neurosci* 2011, **31**:17425–17436.
29. Lin PY, Simon SM, Koh WK, Folorunso O, Umbaugh CS, Pierce A: **Heat shock factor 1 over-expression protects against exposure of hydrophobic residues on mutant SOD1 and early mortality in a mouse model of amyotrophic lateral sclerosis.** *Mol Neurodegener* 2013, **8**:43.
30. Gifondorwa DJ, Robinson MB, Hayes CD, Taylor AR, Prevette DM, Oppenheim RW, Caress J, Milligan CE: **Exogenous delivery of heat shock protein 70 increases lifespan in a mouse model of amyotrophic lateral sclerosis.** *J Neurosci* 2007, **27**:13173–13180.
31. Liu J, Shinobu LA, Ward CM, Young D, Cleveland DW: **Elevation of the Hsp70 chaperone does not effect toxicity in mouse models of familial amyotrophic lateral sclerosis.** *J Neurochem* 2005, **93**:875–882.
32. Mishra A, Maheshwari M, Chhangani D, Fujimori-Tonou N, Endo F, Joshi AP, Jana NR, Yamanaka K: **E6-AP association promotes SOD1 aggresomes degradation and suppresses toxicity.** *Neurobiol Aging* 2013, **34**:1310 e1311-1323.
33. Mishra A, Godavarthi SK, Maheshwari M, Goswami A, Jana NR: **The ubiquitin ligase E6-AP is induced and recruited to aggresomes in response to proteasome inhibition and may be involved in the ubiquitination of Hsp70-bound misfolded proteins.** *J Biol Chem* 2009, **284**:10537–10545.
34. Kumar P, Pradhan K, Karunya R, Ambasta RK, Querfurth HW: **Cross-functional E3 ligases Parkin and C-terminus Hsp70-interacting protein in neurodegenerative disorders.** *J Neurochem* 2012, **120**:350–370.
35. Murata S, Chiba T, Tanaka K: **CHIP: a quality-control E3 ligase collaborating with molecular chaperones.** *Int J Biochem Cell Biol* 2003, **35**:572–578.
36. Cheroni C, Marino M, Tortarolo M, Veglianese P, De Biasi S, Fontana E, Zuccarello LV, Maynard CJ, Dantuma NP, Bendotti C: **Functional alterations of the ubiquitin-proteasome system in motor neurons of a mouse model of familial amyotrophic lateral sclerosis.** *Hum Mol Genet* 2009, **18**:82–96.
37. Borchelt DR, Davis J, Fischer M, Lee MK, Slunt HH, Ratovitsky T, Regard J, Copeland NG, Jenkins NA, Sisodia SS, Price DL: **A vector for expressing foreign genes in the brains and hearts of transgenic mice.** *Genet Anal* 1996, **13**:159–163.
38. Takao K, Miyakawa T: **Light/dark transition test for mice.** *J Vis Exp* 2006, **1**:e104. doi: 10.3791/104
39. Takao K, Yamasaki N, Miyakawa T: **Impact of brain-behavior phenotyping of genetically-engineered mice on research of neuropsychiatric disorders.** *Neurosci Res* 2007, **58**:124–132.
40. Bruijn LI, Becher MW, Lee MK, Anderson KL, Jenkins NA, Copeland NG, Sisodia SS, Rothstein JD, Borchelt DR, Price DL, Cleveland DW: **ALS-linked SOD1 mutant G85R mediates damage to astrocytes and promotes rapidly progressive disease with SOD1-containing inclusions.** *Neuron* 1997, **18**:327–338.

doi:10.1186/s13041-014-0062-1
Cite this article as: Watanabe *et al.*: SIRT1 overexpression ameliorates a mouse model of SOD1-linked amyotrophic lateral sclerosis via HSF1/HSP70i chaperone system. *Molecular Brain* 2014 7:62.

FEBS Open Bio 4 (2014) 1–10

ELSEVIER

CrossMark

FEBS openbio

journal homepage: www.elsevier.com/locate/febsopenbio

1964–2014

The ALS/FTLD-related RNA-binding proteins TDP-43 and FUS have common downstream RNA targets in cortical neurons☆

Daiyu Honda[a], Shinsuke Ishigaki[a,*], Yohei Iguchi[a], Yusuke Fujioka[a], Tsuyoshi Udagawa[a], Akio Masuda[b], Kinji Ohno[b], Masahisa Katsuno[a], Gen Sobue[a,*]

[a] Department of Neurology, Nagoya University Graduate School of Medicine, Nagoya, Japan
[b] Division of Neurogenetics, Center for Neurological Diseases and Cancer, Nagoya University Graduate School of Medicine, Nagoya, Japan

ARTICLE INFO

Article history:
Received 13 August 2013
Received in revised form 11 November 2013
Accepted 11 November 2013

Keywords:
ALS
FTLD
TDP-43
FUS
Transcriptome

ABSTRACT

TDP-43 and FUS are linked to amyotrophic lateral sclerosis (ALS) and frontotemporal lobar degeneration (FTLD), and loss of function of either protein contributes to these neurodegenerative conditions. To elucidate the TDP-43- and FUS-regulated pathophysiological RNA metabolism cascades, we assessed the differential gene expression and alternative splicing profiles related to regulation by either TDP-43 or FUS in primary cortical neurons. These profiles overlapped by >25% with respect to gene expression and >9% with respect to alternative splicing. The shared downstream RNA targets of TDP-43 and FUS may form a common pathway in the neurodegenerative processes of ALS/FTLD.

1. Introduction

Amyotrophic lateral sclerosis (ALS) is a neurodegenerative disorder characterized by the death of motor neurons in the spinal cord, brainstem, and motor cortex [1]. Frontotemporal lobar degeneration (FTLD) is a dementia syndrome characterized by progressive changes in behavior, personality, and/or language resulting from the gradual deterioration of the frontal and temporal lobes [2,3]. Transactive response (TAR) DNA-binding protein 43 (TDP-43) and fused in sarcoma (FUS) have been genetically and pathologically linked to ALS and FTLD; however, the underlying mechanisms by which TDP-43 and FUS induce ALS and FTLD pathologies are unknown [2,3].

TDP-43 was identified as a major component of cytoplasmic neuronal inclusions in sporadic ALS and FTLD patients [4,5], and missense mutations in *TARDBP*, the gene encoding TDP-43, are a known cause of familial ALS and FTLD [6–8]. Familial cases of ALS and FTLD involving TDP-43 mutations and sporadic cases of these diseases exhibit highly similar clinical and pathological characteristics [9], suggesting that TDP-43 plays an important role in the pathogenesis of sporadic ALS and FTLD. Similarly, FUS is also a causative gene for familial ALS and FTLD; in these diseases, redistribution to the cytoplasm and the formation of cytoplasmic aggregates occur for both the TDP-43 and FUS proteins [10,11]. TDP-43 and FUS also share many common pathophysiological characteristics. In particular, these proteins are structurally similar heterogeneous ribonucleoproteins (hnRNPs), as both TDP-43 and FUS are RNA-binding proteins with RNA recognition motifs (RRMs); they are typically predominantly found in the nucleus; their pathological forms are located mainly in the cytosol; and they are involved in transcription, alternative splicing, translation, and RNA transport [12–14].

Although it remains unclear whether a loss of function or gain of toxicity of TDP-43 or FUS is a major cause of ALS/FTLD, the loss of these RNA-binding proteins in the nucleus is a plausible trigger of neurodegeneration. This hypothesis has been supported by several lines of evidence, including the fact that TDP-43 or FUS nuclear staining is lost in the nuclei of neurons in both human ALS/FTLD tissue [15,16] and TDP-43 overexpressing mice [17,18]. In addition, animal models involving the loss of either TDP-43 or FUS mimic the pathology of ALS/FTLD [19–22]. Recently, analyses of TDP-43 using fly models revealed

Abbreviations: ALS, amyotrophic lateral sclerosis; Cugbp1, CUG triplet repeat, RNA-binding protein 1; DAVID, Database for Annotation, Visualization and Integrated Discovery; FTLD, frontotemporal lobar degeneration; FUS, fused in sarcoma; GFAP, glial fibrillary acidic protein; GO, Gene Ontology; hnRNAPs, heterogeneous ribonucleoproteins; LTP, long-term potentiation; RIN, RNA integrity numbers; RMA, robust multichip average; RRMs, RNA recognition motifs; SBMA, spinal and bulbar muscular atrophy; shCont, shRNA/control; shCugbp1, shRNA/Cugbp1; shFUS, shRNA/FUS; shTDP, shRNA/TDP-43; TDP-43, transactive response (TAR) DNA-binding protein 43; TGF, transforming growth factor.

* Corresponding authors. Address: Department of Neurology, Nagoya University Graduate School of Medicine, 65 Tsurumai, Showa-ku, Nagoya 466-8550, Japan. Tel.: +81 52 744 2391; fax: +81 52 744 2785. Tel.: +81 52 744 2385; fax: +81 52 744 2785.
E-mail addresses: ishigaki-ns@umin.net (S. Ishigaki) sobueg@med.nagoya-u.ac.jp (G. Sobue).

2211-5463/$36.00 © 2013 The Authors. Published by Elsevier B.V. on behalf of Federation of European Biochemical Societies. All rights reserved.
http://dx.doi.org/10.1016/j.fob.2013.11.001

that the up- and down-regulation of TDP-43 produced highly similar transcriptome alterations [23]. Cross-rescue analysis in *Drosophila* demonstrated that FUS acted together with and downstream of TDP-43 in a common genetic pathway [21]. Thus, it is intriguing to compare the transcriptome profiles from neurons with silenced TDP-43 or FUS. This experiment could clarify the common molecular mechanisms of ALS/FTLD that are associated with TDP-43 and FUS.

Recently, we investigated the transcriptome profiles of FUS regulation in different cell lineages of the central nervous system and determined that FUS regulates both gene expression and alternative splicing events in a cell-specific manner that is associated with ALS/FTLD [24]. In the current study, we investigated the transcriptome profiles of TDP-43-silenced primary cortical neurons and compared these profiles with the transcriptome profiles of FUS-silenced neurons. The gene expression and alternative splicing event profiles related to regulation by TDP-43 and by FUS were rather similar, suggesting that TDP-43 and FUS may regulate common downstream RNA targets and molecular cascades that could potentially be associated with the pathomechanisms of ALS/FTLD.

2. Methods

2.1. Lentivirus

We designed two different shRNAs against mouse *Tardbp* (*Tdp-43*), *Fus*, and a control shRNA. The targeted sequences were 5′-CGATGAACCCATTGAAATA-3′ for shRNA/TDP-43–1 (shTDP1); 5′-GAGTGGAGGTTATGGTCAA-3′ for shRNA/TDP-43–2 (shTDP2); 5′-GCAACAAAGCTACGGACAA-3′ for shRNA/FUS1 (shFUS1); 5′-GAGTGGAGGTTATGGTCAA-3′ for shRNA/FUS2 (shFUS2); 5′-GGCTTAAAGTGCAGCTCAA-3′ for shRNA/Cugbp1 (shCugbp1); and 5′-AAGCAAAGATGTCTGAATA-3′ for shRNA/control (shCont). The shRNAs were cloned into a lentiviral shRNA vector (pLenti-RNAi-X2 puro DEST, w16–1, which was a kind gift from Dr. Eric Campeau at Resverlogix Corp.). Lentivirus was prepared in accordance with the protocols detailed by Campeau et al. [25].

2.2. Primary cortical neuron culture and the depletion of TDP-43 and FUS

Primary cortical neurons were obtained from the fetal brains of C57BL/6 mouse embryos on embryonic day 15 (E15). The detailed procedure for acquiring these neurons was described in previously published reports [26]. On day 5, neurons were infected with 2×10^{10} copies/well (1.5×10^{7} copies/μl) of lentivirus expressing shRNA against mouse *Tdp-43* (shTDP1 or shTDP2), mouse Cugbp1 (CUG triplet repeat, RNA-binding protein 1) (shCugbp1), or scrambled control (shCont). The virus-containing media was removed at 4 h after infection. The neurons were then cultured for 6 additional days and harvested on day 11 for RNA extraction and cDNA synthesis. Each knockdown experiment was performed in triplicate for each microarray analysis. Experiments were performed in accordance with the Guide for the Care and Use of Laboratory Animals issued by the National Institutes of Health and with the approval of the Nagoya University Animal Experiment Committee (Nagoya, Japan). The experiments on FUS-silenced primary cortical neurons were performed in the manner described above and have been detailed in a previously published report [26].

For immunohistochemical analyses, we used an anti-β-tubulin antibody (TU20, Santa Cruz, Santa Cruz, CA), an anti-glial fibrillary acidic protein (GFAP) antibody (EB4, Enzo Life Sciences, Plymouth Meeting, PA), and 4′,6-diamidino-2-phenylindole (DAPI) staining.

For immunoblot analyses, cells were lysed in TNE buffer containing protease inhibitors for 15 min on ice. The lysates were then cleared by centrifuging the cells at 13,000g for 15 min at 4 °C. Lysates were normalized for total protein (10 μg per lane), separated using a 4–20% linear gradient SDS–PAGE and electroblotted. For immunoblot, we used anti-FUS antibodies (A300–293A, Bethyl Laboratories, Montgomery, TX), anti-TDP-43 antibody (Proteintech, Chicago, IL), and anti-actin antibody (Sigma, St. Louis, MO).

2.3. Microarray analysis

Total RNA was extracted from primary cortical neurons using the RNeasy Mini Kit (Qiagen, Hilden, Germany). We confirmed that the RNA integrity numbers (RIN) for the extracted samples were all greater than 7.0. We synthesized and labeled cDNA fragments from 100 ng of total RNA using the GeneChip WT cDNA Synthesis Kit (Ambion, Austin, TX). Hybridization and signal acquisition for the GeneChip Mouse Exon 1.0 ST Array (Affymetrix, Santa Clara, CA) were performed according to the manufacturer's instructions. Each array experiment was performed in triplicate. The robust multichip average (RMA) and iterative probe logarithmic intensity error (iterPLIER) methods were employed to normalize exon-level and gene-level signal intensities, respectively, using Expression Console 1.1.2 (Affymetrix). We utilized the gene annotation provided by Ensembl version e!61, which is based on the National Center for Biotechnology Information (NCBI) Build 37.1/mm9 of the mouse genome assembly. All microarray data were registered in the Gene Expression Omnibus with accession numbers of GSE36153 (shFUS) and GSE46148 (shTDP-43 and shCugbp1).

Using Student's *t*-test, we compared the gene-level signal intensities from three controls treated with shCont with the gene-level signal intensities of three samples treated with either shTDP1 or shTDP2. We also analyzed alternative splicing profiles by filtering the exon-level signal intensities, using a *t*-test with a threshold of p-value ≤ 0.1. Gene expression and alternative splicing profiles related to FUS regulation in primary cortical neurons were also obtained by comparing gene-level and exon-level signal intensities from three controls treated with shCont with the corresponding signal intensities from three samples treated with either shFUS1 or shFUS2, as previously described [26]. As a control for the RNA-binding protein-silencing model, we analyzed the gene-level and exon-level signal intensities of three samples treated with wither shCugbp1or shCont.

2.4. RT-PCR for alternative splicing analyses

Total RNA was isolated from cells using the RNeasy Mini Kit (Qiagen). The extracted RNA was then treated with DNase I (Qiagen). cDNA was synthesized from 1 μg of total RNA using oligo(dT) primers (Promega, Madison, WI). Primers for each candidate exon were designed using the Primer3 software program (http://frodo.wi.mit.edu/primer3/input.htm). The primer sequences are provided in Supplementary Table 1. Semi-quantitative reverse transcription polymerase chain reaction (RT-PCR) was performed using Ex Taq (Takara Bio Inc., Otsu, Japan), with the following amplification conditions: 25–30 cycles of 98 °C for 10 s, 60 °C for 30 s, and 72 °C for 1 min. The PCR products were electrophoresed on a 15% acrylamide gel and stained with ethidium bromide. The intensity of each band was measured using the Multi Gauge software program (Fujifilm, Tokyo, Japan).

2.5. Real-time qPCR for gene expression analysis

The RNeasy Mini Kit (Qiagen) was used to isolate total RNA from cells; 1 μg of total RNA was then reverse transcribed, using oligo-dT primers. This transcription utilized the CFX96 system (BioRad, Hercules, CA) and thermocycler conditions of 95 °C for 3 min followed by 40 cycles of 95 °C for 10 s and 55 °C for 30 s.

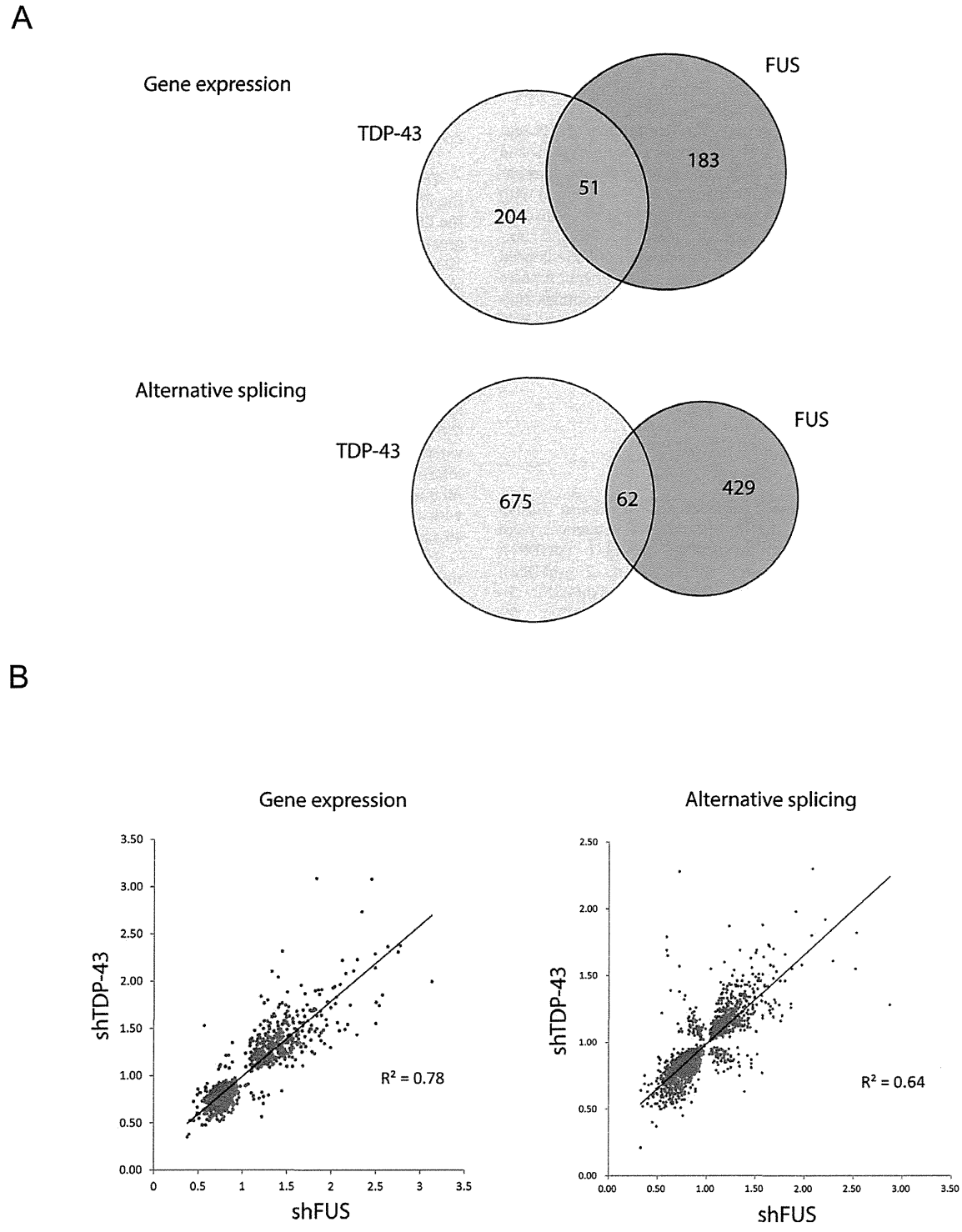

Fig. 1. Comparisons of the gene expression and exon splicing profiles of TDP-43-silenced primary cortical neurons and FUS-silenced primary cortical neurons. (A) Gene expression and alternative splicing profiles of TDP-43-silenced primary cortical neurons- and FUS-silenced primary cortical neurons were compared. Venn diagrams indicate the overlaps in the genes (top) and exons (bottom) with expression levels that were uniquely or concordantly regulated by TDP-43 and/or FUS (t-test, $p < 0.05$; fold change ≤ 0.67 or ≥ 1.5). (B) The fold changes in overlapping genes filtered by t-tests (with a threshold of $p < 0.1$) were plotted for TDP-43-silenced primary cortical neurons and FUS-silenced primary cortical neurons. Scatter plots of the fold changes in gene expression levels (left) and alternative splicing events (right) for shTDP-43 and shFUS. The R^2 value was calculated for genes and exons with t-test p-values <0.1.

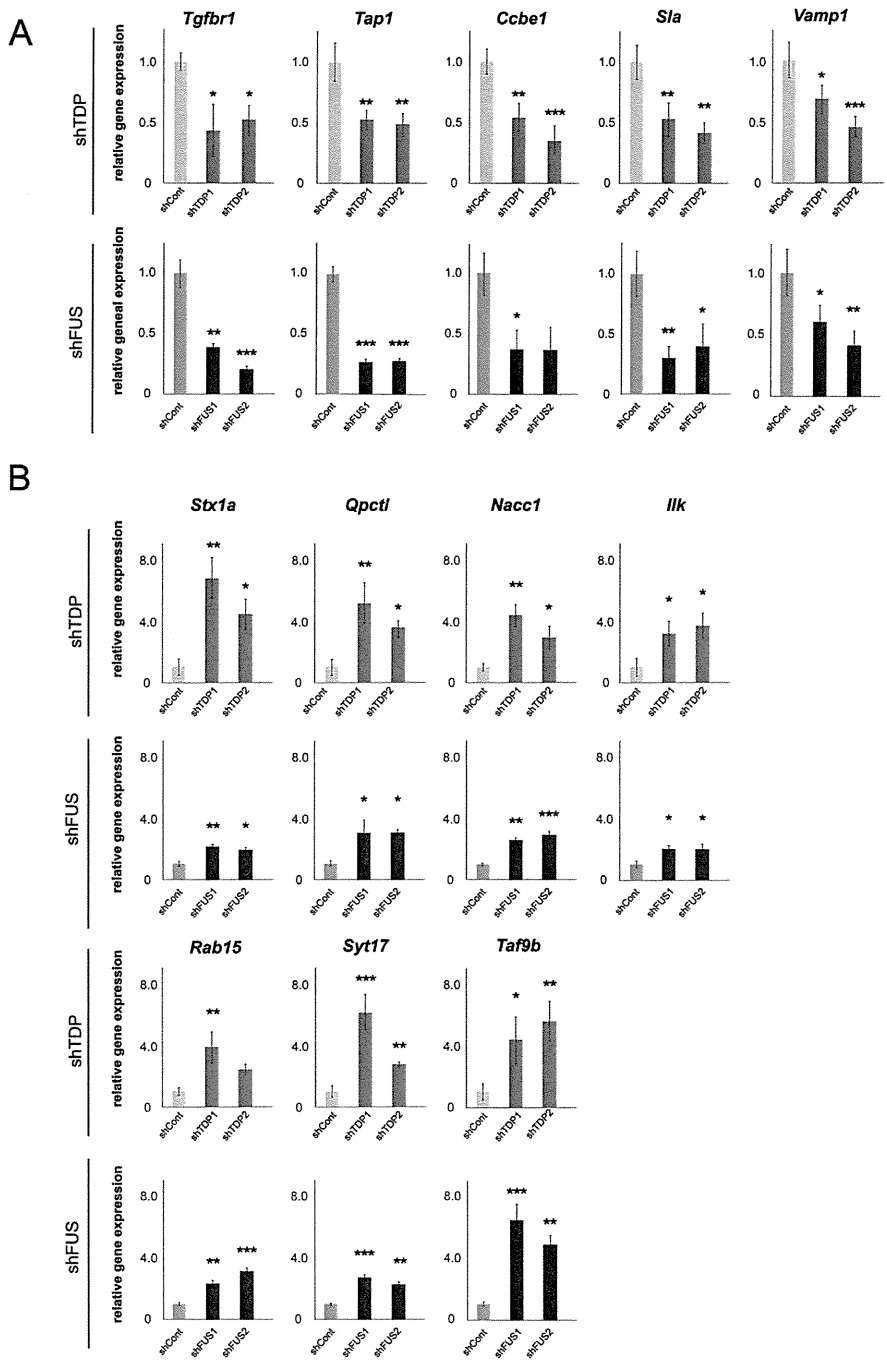

Fig. 2. The validation of differentially expressed genes regulated by both TDP-43 and FUS. Twelve genes with differential expression in both TDP-43-silenced neurons and FUS-silenced neurons in Table 2 were validated by real-time qPCR ($n = 3$; mean and SD). Quantities are calculated by the ratio to β-actin and shown as the relative expression ratio to shCont. Five commonly down-regulated genes (A) and seven commonly up-regulated genes (B) are indicated. Statistics were done by one-way ANOVA and Tukey test. * ($p < 0.05$), ** ($p < 0.01$), and *** ($p < 0.001$) denote significant differences.

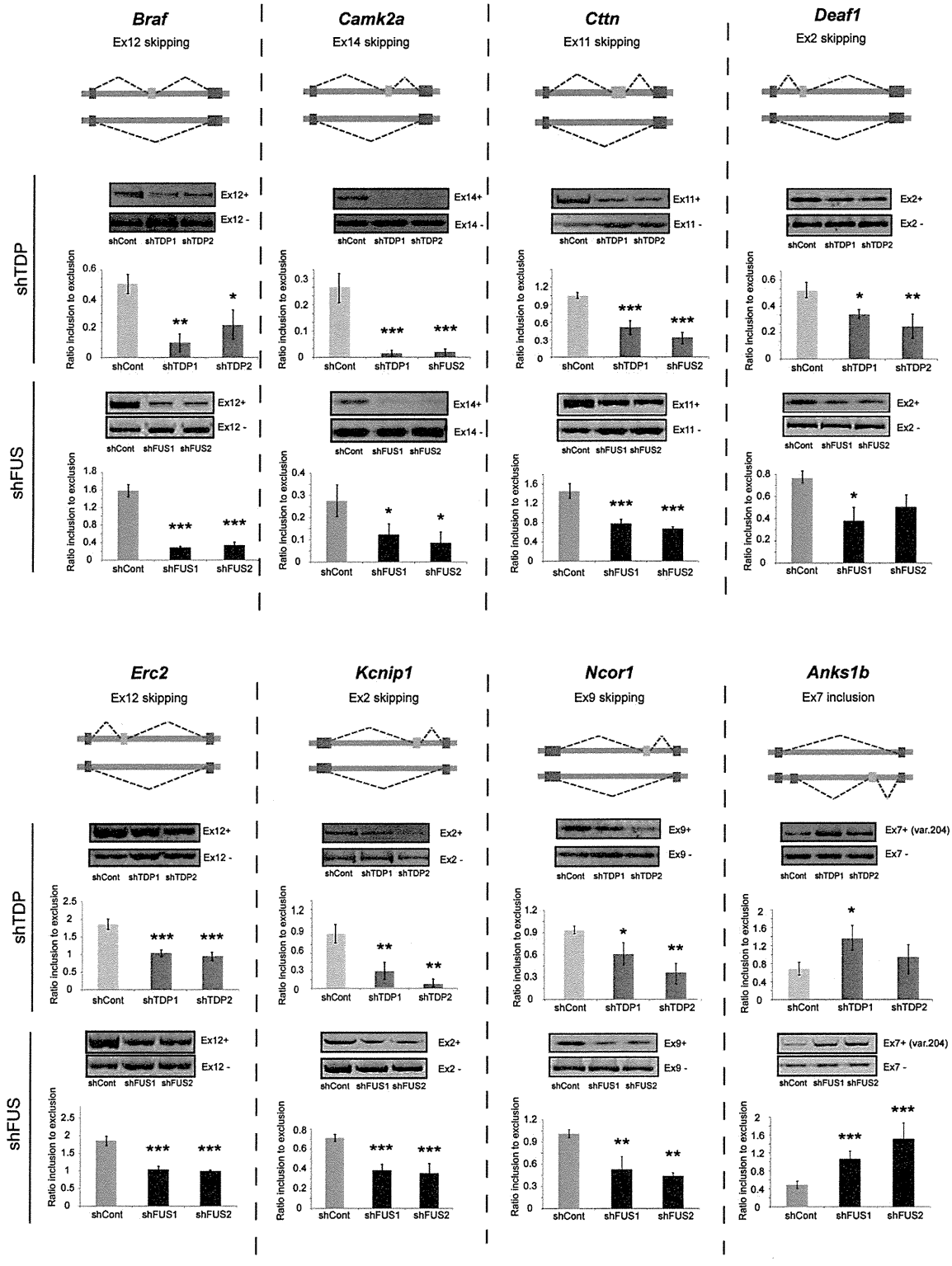

Fig. 3. The validation of representative altered splicing events in TDP-43-silenced primary cortical neurons and FUS-silenced primary cortical neurons. Eight exons with differential expression in both TDP-43-silenced neurons and FUS-silenced neurons were validated by semiquantitative RT-PCR. The top panel provides a schematic of splicing changes mediated by TDP-43 and/or FUS. The second and third panels display representative RT-PCR results for the indicated exons and the densitometric quantification (ratio of inclusion to exclusion) of these results ($n = 3$; mean and SD) after either TDP-43 or FUS depletion. *$p < 0.05$ by t-test. Statistics were done by one-way ANOVA and Tukey test. * ($p < 0.05$), ** ($p < 0.01$), and *** ($p < 0.001$) denote significant differences.

Table 1
Gene Ontology terms for gene expression/alternative splicing in TDP-43- or FUS-silenced neurons.

shTDP-43	Gene expression		shFUS	Gene expression	
GO ID	Term	*p*-Value	GO ID	Term	*p*-Value
GO:0007264	Small GTPase mediated signal transduction	8.37E−07	GO:0019637	Organophosphate metabolic process	3.68E−04
GO:0007242	Intracellular signaling cascade	1.04E−05	GO:0006644	Phospholipid metabolic process	4.89E−04
GO:0044271	Nitrogen compound biosynthetic process	2.98E−04	GO:0016055	Wnt receptor signaling pathway	5.21E−04
GO:0006790	Sulfur metabolic process	9.94E−04	GO:0009100	Glycoprotein metabolic process	5.30E−04
GO:0009100	Glycoprotein metabolic process	0.00169596	GO:0007264	Small GTPase mediated signal transduction	5.91E−04
GO:0009101	Glycoprotein biosynthetic process	0.0019038	GO:0006650	Glycerophospholipid metabolic process	8.42E−04
GO:0018130	Heterocycle biosynthetic process	0.0033067	GO:0007242	Intracellular signaling cascade	0.00122745
GO:0022604	Regulation of cell morphogenesis	0.00426464	GO:0007265	Ras protein signal transduction	0.00389788
GO:0016055	Wnt receptor signaling pathway	0.00455985	GO:0046486	Glycerolipid metabolic process	0.00481341
GO:0031344	Regulation of cell projection organization	0.00619132	GO:0006665	Sphingolipid metabolic process	0.00514754
GO:0043085	Positive regulation of catalytic activity	0.0063261	GO:0030384	Phosphoinositide metabolic process	0.00562443
GO:0031345	Negative regulation of cell projection organization	0.00656187	GO:0006793	Phosphorus metabolic process	0.00563812
GO:0043413	Biopolymer glycosylation	0.00855583	GO:0006796	Phosphate metabolic process	0.00563812
GO:0006486	Protein amino acid glycosylation	0.00855583	GO:0006643	Membrane lipid metabolic process	0.00613362
GO:0070085	Glycosylation	0.00855583	GO:0009101	Glycoprotein biosynthetic process	0.00691847
GO:0010975	Regulation of neuron projection development	0.00912726	GO:0051348	Negative regulation of transferase activity	0.00924863
GO:0030384	Phosphoinositide metabolic process	0.010632	GO:0006600	Creatine metabolic process	0.01095567
GO:0010769	Regulation of cell morphogenesis involved in differentiation	0.01225994	GO:0044242	Cellular lipid catabolic process	0.01200742
GO:0019932	Second-messenger-mediated signaling	0.01617062	GO:0006486	Protein amino acid glycosylation	0.01276803
GO:0050770	Regulation of axonogenesis	0.01657312	GO:0070085	Glycosylation	0.01276803

shTDP-43	Alternative splicing		shFUS	Alternative splicing	
GO ID	Term	*p*-Value	GO ID	Term	*p*-Value
GO:0016192	Vesicle-mediated transport	2.76E−05	GO:0045202	Synapse	6.85E−07
GO:0044057	Regulation of system process	2.41E−04	GO:0042995	Cell projection	2.54E−06
GO:0006936	Muscle contraction	5.09E−04	GO:0043005	Neuron projection	2.29E−05
GO:0003012	Muscle system process	7.75E−04	GO:0005856	Cytoskeleton	1.73E−04
GO:0006897	Endocytosis	0.00107681	GO:0005886	Plasma membrane	1.88E−04
GO:0010324	Membrane invagination	0.00107681	GO:0043232	Intracellular non-membrane-bounded organelle	2.07E−04
GO:0046903	Secretion	0.00244805	GO:0043228	Non-membrane-bounded organelle	2.07E−04
GO:0048167	Regulation of synaptic plasticity	0.00322575	GO:0044456	Synapse part	3.76E−04
GO:0050804	Regulation of synaptic transmission	0.00339707	GO:0030424	Axon	5.70E−04
GO:0050808	Synapse organization	0.00342093	GO:0031252	Cell leading edge	7.01E−04
GO:0043524	Negative regulation of neuron apoptosis	0.0036232	GO:0044463	Cell projection part	7.08E−04
GO:0051969	Regulation of transmission of nerve impulse	0.00432752	GO:0030054	Cell junction	7.20E−04
GO:0006887	Exocytosis	0.00477415	GO:0015630	Microtubule cytoskeleton	0.00738251
GO:0031644	Regulation of neurological system process	0.00525083	GO:0045211	Postsynaptic membrane	0.00825557
GO:0032940	Secretion by cell	0.00587779	GO:0042734	Presynaptic membrane	0.0133955
GO:0006816	Calcium ion transport	0.00667547	GO:0044430	Cytoskeletal part	0.02340953
GO:0016044	Membrane organization	0.0067241	GO:0044459	Plasma membrane part	0.02454379
GO:0046777	Protein amino acid autophosphorylation	0.00788146	GO:0001726	Ruffle	0.03547283
GO:0007628	Adult walking behavior	0.01199082	GO:0032589	Neuron projection membrane	0.04340658
GO:0043523	Regulation of neuron apoptosis	0.01330492	GO:0005938	Cell cortex	0.04544057

The relative quantity of each transcript was calculated by creating a standard curve using the cycle thresholds for serial dilutions of complementary DNA (cDNA) samples, normalized to quantities of β-actin. The PCR was performed in triplicate for each sample, and all experiments were repeated twice. iQ SYBR Green Supermix (BioRad) and the sets of primers listed in Supplementary Table 1 were used for real-time quantitative polymerase chain reaction (qPCR) amplifications.

Table 2
Differentially expressed genes regulated by both TDP-43 and FUS.

Gene symbol	Gene name	shTDP_FC	shFUS_FC
Tgfbr1	Transforming growth factor, beta receptor 1	0.38	0.40
Tap1	Transporter 1, ATP-binding cassette, sub-family B (MDR/TAP)	0.53	0.41
Ccbe1	Collagen and calcium binding EGF domains 1	0.60	0.60
Sla	src-like adaptor	0.61	0.58
Vamp1	Vesicle-associated membrane protein 1	0.66	0.64
Rab15	RAB15, member RAS oncogene family	1.96	2.10
Taf9b	TAF9B RNA polymerase II, TATA box binding protein (TBP)-associated factor	2.00	3.13
Ilk	Integrin-linked kinase	2.08	2.16
Nacc1	Nucleus accumbens associated 1, BEN and BTB (POZ) domain containing	2.29	2.49
Qpctl	Glutaminyl-peptide cyclotransferase-like	2.37	2.63
Syt17	Synaptotagmin 17	3.08	1.82
Stx1a	Syntaxin 1A	3.08	2.45

Table 3
Genes with altered exon splicing regulated by both TDP-43 and FUS.

Gene symbol	Gene name	Spliced site	
Braf	Braf transforming gene	Exon12	Skipping
Camk2a	Calcium/calmodulin-dependent protein kinase II alpha	Exon14	Skipping
Cttn	Cortactin	Exon11	Skipping
Deaf1	Deformed epidermal autoregulatory factor 1	Exon2	Skipping
Erc2	ELKS/RAB6-interacting/CAST family member 2	Exon12	Skipping
Kcnip1	Kv channel-interacting protein 1	Exon2	Skipping
Ncor1	Nuclear receptor corepressor 1	Exon9	Skipping
Anks1b	Ankyrin repeat and sterile alpha motif domain containing 1B	Exon7	Inclusion

3. Results

3.1. The shRNA-mediated silencing of TDP-43 and FUS in primary cortical neurons using lentivirus

To compare the global profiles of RNA molecules regulated by TDP-43 and FUS in primary cortical neurons, we produced TDP-43-silenced primary motor neurons by infecting neurons with lentivirus expressing shRNA against TDP-43; control neurons were produced by infection with lentivirus expressing RNA against a scrambled control. The profiles of FUS-silenced primary cortical neurons using shFUS1 and shFUS2 were established in a previous study [26]. The purity of the primary cortical neurons was confirmed through immunostaining. We successfully established the desired primary cortical neurons with a purity of greater than 95% (Supplementary Fig. S1A).

The expression levels of TDP-43 were suppressed by approximately 60–90% by shTDP1 or shTDP2, as measured by real-time qPCR (Supplementary Fig. S1B). The expression levels of FUS were also suppressed by 80–90% by shFUS1 or shFUS2, as reported previously [26]. The protein levels of TDP-43 were markedly lower in primary neurons infected with shTDP1 and shTDP2 than in neurons infected with the shCont based on the immunoblot analysis (Supplementary Fig. S1C, left). In addition, a reduction in FUS protein levels was observed in primary neurons infected with shFUS1 or shFUS2 (Supplementary Fig. S1C, right).

As a control for the RNA-binding protein-silencing model, we knocked down the Cugbp1 gene in primary cortical neurons and confirmed that this knockdown produced a silencing efficiency of greater than 70% (Supplementary Fig. S2).

3.2. Significant overlap in the transcriptomes of TDP-43-silenced neurons and FUS-silenced neurons

We analyzed gene expression levels and alternative splicing in TDP-43-silenced primary neurons using the Affymetrix GeneChip Mouse Exon 1.0 ST Array (GEO Accession No. GSE46148). We used Student's *t*-test to compare the gene-level signal intensities of three controls treated with shCont with the gene-level signal intensities of three samples treated with either shTDP1 or shTDP2. Among the 21,603 genes on the mouse exon array, 1411 genes had *p*-values ≤ 0.01 for both shTDP1 and shTDP2 treatments in the *t*-tests, and the correlation coefficient between the fold changes of the shTDP1 and shTDP2 treatments was 0.83 (Supplementary Fig. S3A).

We also analyzed alternative splicing profiles by filtering the exon-level signal intensities using a threshold of a *t*-test *p*-value ≤ 0.1. This filtering yielded 4973 exons that were altered by both shTDP1 and shTDP2, with a correlation coefficient of 0.801 (Supplementary Fig. S3B). To identify common effects produced by silencing TDP-43 and silencing FUS, we compiled a list of differentially expressed genes and alternatively spliced exons in primary cortical neurons silenced by shTDP-43 and in primary cortical neurons silenced by shFUS. By applying the threshold of a *t*-test *p*-value of ≤ 0.05 and a fold change of ≤ 0.67 or ≥ 1.5 for both shTDP1 and shTDP2, we obtained 204 genes with altered expression levels upon TDP-43 knockdown. Similarly, 183 genes were obtained for FUS by applying the threshold of a *t*-test *p*-value of ≤ 0.05 and a fold change value of ≤ 0.67 or ≥ 1.5 for both shFUS-1 and shFUS-2. Venn diagrams indicated that the set of genes or exons with expression that were differentially and consistently regulated by FUS markedly overlapped with the corresponding set of genes or exons for TDP-43 (*t*-test, $p < 0.05$). In particular, an overlap

of more than 25% was observed among the gene expression profiles of shTDP-43- and shFUS-treated neurons (Fig. 1A, top panel; 51/204 (25.0%) of the genes for shTDP-43; 51/183 (27.9%) of the genes for shFUS).

We also filtered the exon-level signal intensities by applying a threshold of a *t*-test *p*-value of ≤0.05 and a fold change value of ≤0.67 or ≥1.5. We then determined TDP-43- and FUS-regulated exons as well as the overlap between these exons using the same approach that we applied for gene expression. We obtained 675 TDP-43-regulated genes and 429 FUS-regulated genes with altered exon expression. Venn diagrams indicate that there was an overlap of approximately 10% between the alternative splicing profiles produced by shFUS and the alternative splicing profiles produced by shTDP-43 (Fig. 1A, bottom panel; 61/674 (9.1%) of the genes for shTDP-43; 61/428 (14.3%) of the genes for shFUS).

We then compared the changes in the overlapping genes or exons affected by both shTDP-43 and shFUS after filtering these genes and exons using a *t*-test (with a threshold of $p < 0.1$). The fold change plot analysis demonstrated a strong correlation between shTDP-43 and shFUS with respect to gene expression (Fig. 1B left; $R^2 = 0.78$); in contrast, the gene expression profile for neurons transduced with shRNA targeting a different RNA-binding protein, Cugbp1, did not correlate well with the expression profiles of neurons transduced with shTDP-43 ($R^2 = 0.46$) or shFUS ($R^2 = 0.53$) (Supplementary Fig. S4A). The fold change plot analysis of exon splicing also demonstrated a moderate correlation between shTDP-43 and shFUS (Fig. 1B right; $R^2 = 0.64$). The exon splicing profile for neurons silenced with shRNA against Cugbp1 showed lesser correlation with the exon splicing profiles of neurons transduced with shTDP-43 ($R^2 = 0.52$) or shFUS ($R^2 = 0.48$) (Supplementary Fig. S4B).

We next analyzed the Gene Ontology (GO) terms for the genes that were regulated by TDP-43 and FUS (*t*-test, $p < 0.1$; fold change of ≤0.77 or ≥1.3) using the Database for Annotation, Visualization and Integrated Discovery (DAVID), version 6.7 [27,28]. Genes regulated by TDP-43 were mainly categorized as being involved in signaling cascades and metabolic processes, and the GO terms for these genes were similar to the GO terms for genes regulated by FUS. In the list of the top 20 GO terms for genes with TDP-43-regulated expression and the corresponding list for genes with FUS-regulated expression, we identified eight common GO terms, including "small GTPase-mediated signal transduction" and "Wnt receptor signaling pathway" (Table 1). We also compiled the list of top 20 GO terms for genes with Cugbp1-regulated expression (Supplementary Table S2). Only one and three common GO terms were identified in between the lists of Cugbp1- and TDP-43-regulated expression (GO:0007264) and Cugbp1- and FUS-regulated expression (GO:0007264, 0019637, and 0006644), respectively. In contrast, the GO terms for genes with TDP-43- or FUS-related alternative splicing regulation mainly referred to various neuronal functions; however, none of the same GO terms appeared in both the list of the top 20 GO terms for genes with TDP-43-regulated alternative splicing and the corresponding list for genes with FUS-regulated alternative splicing (Table 1).

3.3. Gene expression profiles are similar among the top 20 genes regulated by TDP-43 and FUS

We next investigated the detailed gene expression profiles of TDP-43-silenced primary cortical neurons. By filtering gene-level signal intensities using a *t*-test (with a threshold of *p*-value ≤0.1) and fold change (which was required to be ≤0.67 or ≥1.5), genes with differential expression in TDP-43-silenced primary cortical neurons were selected. Fourteen of the top 20 genes with expression regulated by TDP-43 were also regulated by FUS (Supplementary Table S3). To select genes with differential expression upon changes in FUS regulation, gene-level signal intensities in the profile of FUS-silenced primary cortical neurons were filtered using a *t*-test (with a threshold of *p*-value ≤0.1) and fold change (which was required to be ≤0.67 or ≥1.5). Genes that were differentially expressed in both TDP-43-silenced primary cortical neurons and FUS-silenced primary cortical neurons (as determined by the *p*-value ≤0.1 and fold change of ≤0.67 or ≥1.5 requirements) are listed with their fold change values in Table 2. The list of commonly regulated genes includes 12 genes: five downregulated genes, such as *Tgfbr1* (transforming growth factor-β receptor I; Fig. 2A), and seven upregulated genes, such as *Stx1a* (syntaxin 1A; Fig. 2B). The results were validated using quantitative reverse transcription polymerase chain reaction (qRT-PCR) and shown as mRNA expression ratio to β-actin (Fig. 2) and Gapdh (Supplementary Fig. S5).

3.4. Genes with altered exon splicing regulated by both TDP-43 and FUS

After filtering the exons in genes that were differentially expressed in both shTDP1- and shTDP2-treated neurons, using the threshold of a *t*-test *p*-value of ≤0.1 and a fold change of ≥1.3 in primary neurons, we compared these exons with the profiles of alternatively spliced exons in shFUS1 and shFUS2 to obtain genes with altered splicing events that were commonly regulated by both TDP-43 and FUS. After validation by RT-PCR, we obtained 8 exons with alternative splicing events regulated by both TDP-43 and FUS (Table 3 and Fig. 3).

4. Discussion

Both TDP-43 and FUS are involved in multiple levels of RNA processing, and mutations in these two genes are responsible for familial ALS and FTLD. Although TDP-43 and FUS pathologies appear to largely be mutually exclusive, the molecular and functional similarities between these two molecules suggest that TDP-43 and FUS may share a common downstream pathway leading to neuronal degeneration [29,30].

Genes with altered expression levels or alternatively spliced exons in both TDP-43- and FUS-silenced primary neurons have fundamental functions in neurons, suggesting that transcriptome changes produced by loss-of-function mutations of TDP-43 and/or FUS may lead to neuronal cell death. This conjecture is supported by cross-rescue findings from fish and fly models in which FUS overexpression rescued the defect phenotype caused by TDP-43 knockout [20,21].

How do TDP-43 and FUS regulate common downstream genes and exons? These proteins do not appear to share the same binding target RNAs in neuronal tissue; in particular, it has been reported that the consensus sequences of TDP-43 are (UG) repeats [31,32], whereas FUS has a widespread RNA binding pattern [26,33]. Research has indicated that these two RNA binding proteins may target distinct sets of cytoplasmic mRNA molecules in NSC-34 cells [34]. Although we found that there was an overlap of approximately 10% between genes with altered splicing after shFUS treatment and genes with altered splicing after shTDP-43 treatment, the regulation mechanism of common alternative splicing events remains unclear.

Our results indicated that 25% of genes with altered gene expression levels and 10% of genes with alternatively spliced exons were common to the transcriptome profiles of both TDP-43-silenced primary cortical neurons and FUS-silenced primary cortical neurons. These findings were comparable to the results reported by Lagier-Tourenne et al., which demonstrated that in adult mouse striatum, there was an overlap of more than 10% between alternative splicing events observed due to TDP-43 knockdown and alternative splicing events observed due to FUS knockdown [35]. Discrepancies between this prior study and the current investigation with respect to targeted RNAs could reflect the different cell types used in these studies; we specifically assessed neurons, whereas the mouse striatum contains a variety of cells, including neurons, glial cells, and other cell types.

In fact, in a recent study, we found distinct FUS-regulated transcriptomes among different cell lineages [24].

Among the target RNA molecules that we identified, *Stx1A* is one of the most differentially upregulated genes in both TDP-43-silenced neurons and FUS-silenced neurons (Table 2). Stx1A encodes Syntaxin 1A, which is a member of the syntaxin super family that is associated with the vesicle fusion process as a component of the SNARE complex [36]. The overexpression of Stx1A disturbed synaptic vesicle exocytosis in hippocampal neurons [37], suggesting that up-regulation of Stx1A by silencing TDP-43 or FUS may produce synaptic dysfunction. *Tgfbr1* is one of the most significantly downregulated genes in both TDP-43-silenced neurons and FUS-silenced neurons (Table 2). Tgfbr1 encodes transforming growth factor (TGF)-β receptor I, which binds to TGF-β and transduces TGF-β signals from the cell surface to the cytoplasm. TGF-β signaling was disrupted in the motor neurons of mouse models of ALS and spinal and bulbar muscular atrophy (SBMA) [38,39]. This finding, in combination with our results, suggests that the TGF-β signaling pathway may be a strong candidate for targeted molecular therapy for motor neuron degeneration.

In addition, exon 14 of the *Camk2a* gene, which encodes the calcium/calmodulin-dependent protein kinase type II α chain, was skipped in both TDP-43-silenced primary neurons and FUS-silenced primary neurons. *Camk2a* is a critical player in calmodulin-dependent activity, long-term potentiation (LTP), and learning [40]. The expression of Camk2a has been reported to be decreased in Alzheimer's patients [41]. Clarifying the role of exon 14 of Camk2a in the function of this protein might link the calmodulin-dependent pathway to TDP-43- and FUS-associated FTLD. Despite the discovery of considerable evidence linking alternative splicing and various diseases, including neurodegeneration, it remains unclear how much alternative splicing is "noise" and how much of this splicing truly contributes to cell fate [42]. Further verification of whether these altered splicing events have pathogenic roles is required.

In this study, we determined that TDP-43-silenced neurons and FUS-silenced neurons exhibited greater overlap in shared gene expression alterations than in altered splicing events. In addition, a considerable number of GO terms from gene expression data were common to both types of neurons, whereas distinct GO terms were obtained from alternative splicing events in the two types of neurons. These results suggest that TDP-43 and FUS do not share many splicing targets but instead may associate with each other during mRNA maturation and/or transportation, resulting in altered gene expression. Another possibility is that TDP-43 and FUS may share common molecular pathways that lead to neuronal cell death after multiple transcriptome disturbances.

In summary, the comparative analysis of the transcriptome profiles in primary cortical neurons revealed common downstream RNA targets of TDP-43 and FUS. These targets may be linked to a common pathway in the neurodegenerative processes of ALS/FTLD.

Acknowledgments

Part of this study represents the results of the "Integrated Research on Neuropsychiatric Disorders" project, which has been conducted under the Strategic Research Program for Brain Sciences of the Ministry of Education, Culture, Sports, Science and Technology of Japan. This work was also supported by grants-in-aid from the CREST/JST, MEXT, and MHLW of Japan.

Supplementary material

Supplementary material associated with this article can be found, in the online version, at doi:10.1016/j.fob.2013.11.001.

References

[1] Rothstein, J.D. (2009) Current hypotheses for the underlying biology of amyotrophic lateral sclerosis. Ann. Neurol. 65(Suppl. 1), S3–S9.
[2] Al-Chalabi, A., Jones, A., Troakes, C., King, A., Al-Sarraj, S. and van den Berg, L.H. (2012) The genetics and neuropathology of amyotrophic lateral sclerosis. Acta Neuropathol. 124, 339–352.
[3] Baloh, R.H. (2012) How do the RNA-binding proteins TDP-43 and FUS relate to amyotrophic lateral sclerosis and frontotemporal degeneration, and to each other? Curr. Opin. Neurol. 25, 701–707.
[4] Arai, T. (2006) TDP-43 is a component of ubiquitin-positive tau-negative inclusions in frontotemporal lobar degeneration and amyotrophic lateral sclerosis. Biochem. Biophys. Res. Commun 351, 602–611.
[5] Neumann, M. (2006) Ubiquitinated TDP-43 in frontotemporal lobar degeneration and amyotrophic lateral sclerosis. Science 314, 130–133.
[6] Gitcho, M.A. (2008) TDP-43 A315T mutation in familial motor neuron disease. Ann. Neurol. 63, 535–538.
[7] Sreedharan, J. (2008) TDP-43 mutations in familial and sporadic amyotrophic lateral sclerosis. Science 319, 1668–1672.
[8] Kabashi, E. (2008) TARDBP mutations in individuals with sporadic and familial amyotrophic lateral sclerosis. Nat. Genet. 40, 572–574.
[9] Yokoseki, A. (2008) TDP-43 mutation in familial amyotrophic lateral sclerosis. Ann. Neurol. 63, 538–542.
[10] Kwiatkowski, T.J. Jr. (2009) Mutations in the FUS/TLS gene on chromosome 16 cause familial amyotrophic lateral sclerosis. Science 323, 1205–1208.
[11] Vance, C. (2009) Mutations in FUS, an RNA processing protein, cause familial amyotrophic lateral sclerosis type 6. Science 323, 1208–1211.
[12] Buratti, E. and Baralle, F.E. (2012) TDP-43: gumming up neurons through protein–protein and protein–RNA interactions. Trends Biochem. Sci. 37, 237–247.
[13] Lagier-Tourenne, C. and Cleveland, D.W. (2009) Rethinking ALS: the FUS about TDP-43. Cell 136, 1001–1004.
[14] Strong, M.J. and Volkening, K. (2011) TDP-43 and FUS/TLS: sending a complex message about messenger RNA in amyotrophic lateral sclerosis? FEBS J. 278, 3569–3577.
[15] Davidson, Y., Kelley, T., Mackenzie, I.R., Pickering-Brown, S., Du Plessis, D., Neary, D. et al. (2007) Ubiquitinated pathological lesions in frontotemporal lobar degeneration contain the TAR DNA-binding protein, TDP-43. Acta Neuropathol. 113, 521–533.
[16] Neumann, M., Rademakers, R., Roeber, S., Baker, M., Kretzschmar, H.A. and Mackenzie, I.R. (2009) A new subtype of frontotemporal lobar degeneration with FUS pathology. Brain 132, 2922–2931.
[17] Wegorzewska, I., Bell, S., Cairns, N.J., Miller, T.M. and Baloh, R.H. (2009) TDP-43 mutant transgenic mice develop features of ALS and frontotemporal lobar degeneration. Proc. Natl. Acad. Sci. USA 106, 18809–18814.
[18] Igaz, L.M. (2011) Dysregulation of the ALS-associated gene TDP-43 leads to neuronal death and degeneration in mice. J. Clin. Invest. 121, 726–738.
[19] Iguchi, Y. (2013) Loss of TDP-43 causes age-dependent progressive motor neuron degeneration. Brain 136, 1371–1382.
[20] Kabashi, E., Bercier, V., Lissouba, A., Liao, M., Brustein, E., Rouleau, G.A. et al. (2011) FUS and TARDBP but not SOD1 interact in genetic models of amyotrophic lateral sclerosis. PLoS Genet. 7, e1002214.
[21] Wang, J.W., Brent, J.R., Tomlinson, A., Shneider, N.A. and McCabe, B.D. (2011) The ALS-associated proteins FUS and TDP-43 function together to affect Drosophila locomotion and life span. J. Clin. Invest. 121, 4118–4126.
[22] Wu, L.S., Cheng, W.C. and Shen, C.K. (2012) Targeted depletion of TDP-43 expression in the spinal cord motor neurons leads to the development of amyotrophic lateral sclerosis-like phenotypes in mice. J. Biol. Chem. 287, 27335–27344.
[23] Vanden Broeck, L. (2013) TDP-43 loss-of-function causes neuronal loss due to defective steroid receptor-mediated gene program switching in Drosophila. Cell Rep. 3, 160–172.
[24] Fujioka, Y. (2013) FUS-regulated region- and cell-type-specific transcriptome is associated with cell selectivity in ALS/FTLD. Sci. Rep. 3, 2388.
[25] Campeau, E. (2009) A versatile viral system for expression and depletion of proteins in mammalian cells. PLoS One 4, e6529.
[26] Ishigaki, S. (2012) Position-dependent FUS-RNA interactions regulate alternative splicing events and transcriptions. Sci. Rep. 2, 529.
[27] Huang da, W., Sherman, B.T. and Lempicki, R.A. (2009) Systematic and integrative analysis of large gene lists using DAVID bioinformatics resources. Nat. Protoc. 4, 44–57.
[28] Dennis, G. Jr., Sherman, B.T., Hosack, D.A., Yang, J., Gao, W., Lane, H.C. et al. (2003) DAVID: Database for Annotation, Visualization, and Integrated Discovery. Genome Biol. 4, P3.
[29] Van Langenhove, T., van der Zee, J. and Van Broeckhoven, C. (2012) The molecular basis of the frontotemporal lobar degeneration-amyotrophic lateral sclerosis spectrum. Ann. Med. 44, 817–828.
[30] Polymenidou, M., Lagier-Tourenne, C., Hutt, K.R., Bennett, C.F., Cleveland, D.W. and Yeo, G.W. (2012) Misregulated RNA processing in amyotrophic lateral sclerosis. Brain Res. 1462, 3–15.
[31] Polymenidou, M. (2011) Long pre-mRNA depletion and RNA missplicing contribute to neuronal vulnerability from loss of TDP-43. Nat. Neurosci. 14, 459–468.
[32] Sephton, C.F. (2011) Identification of neuronal RNA targets of TDP-43-containing ribonucleoprotein complexes. J. Biol. Chem. 286, 1204–1215.
[33] Rogelj, B. (2012) Widespread binding of FUS along nascent RNA regulates alternative splicing in the brain. Sci. Rep. 2, 603.

[34] Colombrita, C., Onesto, E., Megiorni, F., Pizzuti, A., Baralle, F.E., Buratti, E. et al. (2012) TDP-43 and FUS RNA-binding proteins bind distinct sets of cytoplasmic messenger RNAs and differently regulate their post-transcriptional fate in motoneuron-like cells. J. Biol. Chem. 287, 15635–15647.
[35] Lagier-Tourenne, C. (2012) Divergent roles of ALS-linked proteins FUS/TLS and TDP-43 intersect in processing long pre-mRNAs. Nat. Neurosci. 15, 1488–1497.
[36] Sorensen, J.B. (2005) SNARE complexes prepare for membrane fusion. Trends Neurosci. 28, 453–455.
[37] Mitchell, S.J. and Ryan, T.A. (2005) Munc18-dependent regulation of synaptic vesicle exocytosis by syntaxin-1A in hippocampal neurons. Neuropharmacology 48, 372–380.
[38] Nakamura, M., Ito, H., Wate, R., Nakano, S., Hirano, A. and Kusaka, H. (2008) Phosphorylated Smad2/3 immunoreactivity in sporadic and familial amyotrophic lateral sclerosis and its mouse model. Acta Neuropathol. 115, 327–334.
[39] Katsuno, M. (2010) Disrupted transforming growth factor-beta signaling in spinal and bulbar muscular atrophy. J. Neurosci. 30, 5702–5712.
[40] Giese, K.P., Fedorov, N.B., Filipkowski, R.K. and Silva, A.J. (1998) Autophosphorylation at Thr286 of the alpha calcium–calmodulin kinase II in LTP and learning. Science 279, 870–873.
[41] Wang, Y.J., Chen, G.H., Hu, X.Y., Lu, Y.P., Zhou, J.N. and Liu, R.Y. (2005) The expression of calcium/calmodulin-dependent protein kinase II-alpha in the hippocampus of patients with Alzheimer's disease and its links with AD-related pathology. Brain Res. 1031, 101–108.
[42] Kornblihtt, A.R., Schor, I.E., Allo, M., Dujardin, G., Petrillo, E. and Munoz, M.J. (2013) Alternative splicing: a pivotal step between eukaryotic transcription and translation. Nat. Rev. Mol. Cell Biol. 14, 153–165.

Available online at www.sciencedirect.com
ScienceDirect
www.elsevier.com/locate/brainres
Brain Research

Research Report

The molecular link between inefficient GluA2 Q/R site-RNA editing and TDP-43 pathology in motor neurons of sporadic amyotrophic lateral sclerosis patients

Takenari Yamashita[a,b], *Shin Kwak*[a,b,c,*]

[a]CREST, *Japan Science and Technology Agency, Japan*
[b]*Center for Disease Biology and Integrative Medicine, Graduate School of Medicine, The University of Tokyo, 7-3-1 Hongo, Bunkyo-ku, Tokyo 113-0033, Japan*
[c]*Clinical Research Center for Medicine, International University of Health and Welfare, Ichikawa, Chiba, 272-0827 Japan*

ARTICLE INFO

Article history:
Accepted 7 December 2013
Available online 16 December 2013

Keywords:
TAR DNA binding protein of 43 kDa (TDP-43)
Calpain
AMPA receptor
GluA2
RNA editing
Adenosine deaminase acting on RNA 2 (ADAR2)
Amyotrophic lateral sclerosis (ALS)

ABSTRACT

TAR DNA-binding protein (TDP-43) pathology and reduced expression of adenosine deaminase acting on RNA 2 (ADAR2), which is the RNA editing enzyme responsible for adenosine-to-inosine conversion at the GluA2 glutamine/arginine (Q/R) site, concomitantly occur in the same motor neurons of amyotrophic lateral sclerosis (ALS) patients; this finding suggests a link between these two ALS-specific molecular abnormalities. AMPA receptors containing Q/R site-unedited GluA2 in their subunit assembly are Ca^{2+}-permeable, and motor neurons lacking ADAR2 undergo slow death in conditional ADAR2 knockout (AR2) mice, which is a mechanistic ALS model in which the ADAR2 gene is targeted in cholinergic neurons. Moreover, deficient ADAR2 induced mislocalization of TDP-43 similar to TDP-43 pathology seen in the sporadic ALS patients in the motor neurons of AR2 mice. The abnormal mislocalization of TDP-43 specifically resulted from activation of the Ca^{2+}-dependent serine protease calpain that specifically cleaved TDP-43 at the C-terminal region, and generated aggregation-prone N-terminal fragments. Notably, the N-terminal fragments of TDP-43 lacking the C-terminus were demonstrated in the brains and spinal cords of ALS patients. Because normalization of either the Ca^{2+}-permeability of AMPA receptors or the calpain activity in the motor neurons normalized the subcellular localization of TDP-43 in AR2 mice, it is likely that exaggerated calpain-dependent TDP-43 fragments played a role at least in the initiation of TDP-43 pathology. Elucidation of the molecular cascade of neuronal death induced by ADAR2 downregulation could provide a new specific therapy for sporadic ALS. In this review, we summarized the work from our group on the role of inefficient GluA2 Q/R site-RNA editing and TDP-43 pathology in

*Corresponding author at: Center for Disease Biology and Integrative Medicine, Graduate School of Medicine, The University of Tokyo, 7-3-1 Hongo, Bunkyo-ku, Tokyo 113-0033, Japan. Fax: +81 3 5841 3566.
E-mail address: kwak-tky@umin.ac.jp (S. Kwak).

http://dx.doi.org/10.1016/j.brainres.2013.12.011

sporadic ALS, and discussed possible effects of inefficient ADAR2-mediated RNA editing in general.

This article is part of a Special Issue entitled RNA Metabolism 2013.

1. ALS and causative genes

Amyotrophic lateral sclerosis (ALS) is the most common adult-onset motor neuron disease affecting healthy middle-aged individuals. The disease course is rapidly progressive, and the eventual respiratory muscle weakness results in death within a few years of onset. More than 90% of ALS cases are sporadic in which the cause of ALS is largely unknown. The remaining cases of ALS are familial (approximately 5–10% of all ALS cases), in approximately half of these cases mutations in several genes have been demonstrated. At present, more than 20 different mutant genes are known to cause familial ALS (Ferraiuolo et al., 2011; Rademakers and van Blitterswijk, 2013), including *SOD1* (Rosen et al., 1993), chromosome 9 open reading frame 72 (*C9ORF72*) (DeJesus-Hernandez et al., 2011; Renton et al., 2011), TAR DNA-binding protein (*TARDBP*) (Gitcho et al., 2008; Kabashi et al., 2008; Sreedharan et al., 2008; Van Deerlin et al., 2008; Yokoseki et al., 2008), Fused in sarcoma (*FUS*) (Kwiatkowski et al., 2009; Vance et al., 2009). These genes account for about 50% of all familial ALS cases (Ferraiuolo et al., 2011), while only a small percentage of sporadic ALS cases had mutations found in these genes. Therefore, it is likely that multiple different molecular mechanisms underlie sporadic ALS and each familial ALS that are associated with different individual causative genes; TDP-43 is a pathological hallmark of the majority of ALS patients, and both TDP-43 pathology and inefficient editing of the GluA2 Q/R site occur concomitantly in many of the motor neurons of patients with sporadic ALS (Aizawa et al., 2010). In *TARDBP*-associated ALS, although TDP-43 pathology is the pathological characteristics as in sporadic ALS that carry wild-type *TARDBP* gene, ADAR2 downregulation has not been demonstrated. Likewise, neither of these two abnormalities were observed in the motor neurons of *SOD1*-associated ALS patients or *SOD1* transgenic animals (Kawahara et al., 2006; Mackenzie et al., 2007; Robertson et al., 2007; Tan et al., 2007). Therefore, elucidation of pathogenic mechanisms specific for sporadic ALS and individual familial ALS cases will be necessary to develop new gene-targeting therapeutic strategies.

2. Abnormal RNA editing and ADAR2 in sporadic ALS motor neurons

GluA2 (previously called GluR2 or GluR-B) is a subunit of the L-α-amino-3-hydroxy-5-methyl-4-isoxazolepropionic acid (AMPA) receptor and pre-mRNA of GluA2 is normally subjected to RNA editing at the glutamine/arginine (Q/R) site. The adenosine at the Q/R site of GluA2 pre-mRNA is converted to inosine (A-to-I conversion) and the genomic CAG codon for Q is converted to a CIG codon in mRNA, and CIG is read as CGG, which is a codon for R during translation. Additionally, because the A-to-I conversion invariably occurs at the Q/R site, all of the GluA2 mRNA expressed in neurons is edited to an R at this site (GluA2R) (Kawahara et al., 2004; Sommer et al., 1991; Takuma et al., 1999).

In the spinal motor neurons of the majority of sporadic ALS patients, RNA editing of GluA2 is inefficient at the glultamine/arginine (Q/R) site, and abnormal Q/R site-unedited GluA2 (GluA2Q) is expressed in approximately half of remaining motor neurons in an individual patient (Hideyama et al., 2012b; Kawahara et al., 2004; Takuma et al., 1999). The expression of GluA2Q in motor neurons has been demonstrated in the majority of sporadic ALS patients so far examined (>30 cases) irrespective of the difference in clinical manifestations (Hideyama et al., 2012b), whereas motor neurons from control subjects and patients with other diseases, including other motor neurons diseases, including spinal and bulbar muscular atrophy and *SOD1*-associated ALS do not express GluA2Q (Kawahara et al., 2006).

Functional AMPA receptors are homo- or hetero-tetramers of four subunits called GluA1–GluA4. The nucleotide sequence in the genomic Q/R site is CAG (a codon for Q) in all of AMPA receptor subunits, and only GluA2 expresses R at the Q/R site resulting from A-to-I conversion (Seeburg, 2002). AMPA receptors are either Ca^{2+}-permeable or -impermeable, which is determined by whether the AMPA receptor has GluA2R in its subunit or not; only the AMPA receptors having GluA2R is Ca^{2+}-impermeable, whereas those composed of only Q/R site-unedited subunits, including GluA2Q are Ca^{2+}-permeable (Seeburg, 2002). A-to-I conversion at the GluA2 Q/R site occurs in all GluA2 expressed in neurons and virtually all neurons in the mammalian brain express only GluA2R (Seeburg, 2002). Additionally, failure of Q-to-R conversion at this site produces Ca^{2+}-permeable AMPA receptors that results in increased excitation of neurons, which has been shown to culminate in fatal status epilepticus in mice (Brusa et al., 1995; Feldmeyer et al., 1999; Higuchi et al., 2000).

Adenosine deaminase acting on RNA 2 (ADAR2) specifically catalyzes the A-to-I conversion at the Q/R site of GluA2 pre-mRNA (Higuchi et al., 1993, 2000). In mammals, there are three structurally related members (ADAR1, ADAR2 and ADAR3) in the ADAR family. ADARs possess two or three double strand RNA binding domains in the N-terminal region and one deaminase domain in the C-terminal region (Hogg et al., 2011). Although ADAR1 and ADAR2 actively catalyze A-to-I conversion with different substrate spectra, ADAR3 that is specifically expressed in the brain, predominantly in the white matter, exhibits no editing activity in either naturally occurring or artificial substrates (Chen et al., 2000; Melcher et al., 1996).

In accordance with these studies on mammalian brains, a recent study demonstrated that the expression levels of ADAR2, but not of ADAR1 or ADAR3, were significantly

decreased in the motor neurons of sporadic ALS patients compared to normal and disease control cases (Hideyama et al., 2012b). Previous studies on gene expression in a global scale has not demonstrated the reduction of ADAR2 gene expression in ALS motor neurons (Jiang et al., 2005), presumably due to the technical reasons. The reduction of ADAR2 expression was extensive in ALS motor neurons expressing GluA2Q, and mild but significant in those expressing only GluA2R (Hideyama et al., 2012b). These results indicate that ADAR2 downregulation is a selective, profound and disease-specific pathological change in motor neurons from sporadic ALS patients.

Recently, by using global genome wide and RNA sequencing analysis, it is now recognized that ADAR2 is involved in the editing of a large number of RNAs including GluA2 (Cattenoz et al., 2013; Li et al., 2009; Maas et al., 2011; Peng et al., 2012; Zhu et al., 2013). The reduction of ADAR2 in motor neurons from ALS patients may induce various defects, including the potential alteration in the role for RNA splicing (Solomon et al., 2013) and control of neuronal excitability (Li et al., 2013). Furthermore, hnRNP A2/B1, known as an enhancer of RNA editing (Garncarz et al., 2013), was recently reported to link to ALS and frontotemporal dementia (FTD) (Kim et al., 2013). Although the functional significance is not clear, there is a report regarding association of ALS and abnormal editing of the glutamate transporter EAAT2, of which downregulation was previously discussed for the pathogenic role in ALS (Flomen and Makoff, 2011). These reports may also suggest the role of altered RNA editing in the pathogenesis of ALS.

3. Abnormal RNA editing and motor neuron death

Pathogenic roles of inefficient RNA editing at the GluA2 Q/R site for sporadic ALS have been demonstrated in the motor neuron-selective conditional ADAR2 knockout (AR2) mice carrying floxed ADAR2 alleles that are targeted by Cre expressed under the control of vesicular acetylcholine transporter (VAChT) promotor (Hideyama et al., 2010). These AR2 mice displayed a slow and progressive motor dysfunction attributable to loss of ADAR2-lacking motor neurons and their neuromuscular motor units. Because the expression of GluA2R by genetic engineering of the endogenous GluA2 gene rescued ADAR2-lacking motor neurons from death in AR2 mice, these results indicate that the death of motor neurons was caused by a Ca^{2+}-permeable AMPA receptor-mediated mechanism resulting from inefficient RNA editing at the GluA2 Q/R site (Hideyama et al., 2010). In heterozygous AR2 (AR2H) mice in which one ADAR2 gene allele was ablated in motor neurons, the motor neurons with reduced ADAR2 expressed GluA2Q mRNA, although to a lesser extent compared to ADAR2-lacking motor neurons in homozygous AR2 mice, and underwent a slow death when examined at 12 months of age (Hideyama and Kwak, 2011).

Taken together, expression of GluA2Q, even if it is a small proportion of all AMPA receptors, is not favorable for the survival of motor neurons in mice and expression of ADAR2 at a level sufficient to edit all of the GluA2 mRNA rather than the expression level of ADAR2 *per se* is the critical factor for motor neuron survival. The critical role of GluA2 Q/R site-editing in neuronal death in mice indicates the pathogenic role of GluA2Q expression in ALS motor neurons (Hideyama et al., 2010). Therefore, insufficient levels of ADAR2 that leads to the expression of GluA2Q are a likely cause of death of motor neurons in sporadic ALS.

4. TDP-43 and RNA editing

The abnormal processing and mislocalization of TAR DNA-binding protein-43 (TDP-43) in motor neurons is known as a pathological hallmark of sporadic ALS (Arai et al., 2006; Neumann et al., 2006) (Fig. 1). TDP-43 is a nuclear protein involved in the regulation of RNA processing (Buratti and

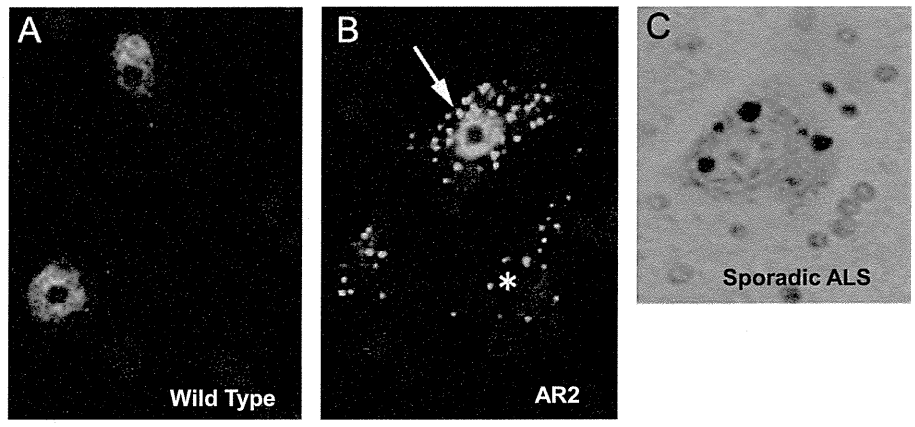

Fig. 1 – TDP-43 is mislocalized in motor neurons lacking ADAR2 in conditional ADAR2 knockout mice (AR2): (A) spinal motor neurons of wild-type mice exhibiting nuclear TDP-43 (green). (B) Immunohistochemistry for TDP-43 in the spinal cord of an AR2 mouse. Numerous TDP-43-positive aggregates in the cytoplasm (arrow) and a reduction or absence (asterisk) of TDP-43 in the nucleus (blue) of motor neurons. TOPRO-3 is a cellular maker (blue). (C) TDP-43 pathology in patients with sporadic ALS, indicating abnormal cytoplasmic inclusions positive for phosphorylated TDP-43.

Baralle, 2010; Colombrita et al., 2012; Daoud et al., 2009; Gendron and Petrucelli, 2011; Iguchi et al., 2009; Johnson et al., 2009; Nonaka et al., 2009; Polymenidou et al., 2011; Sephton et al., 2011; Tollervey et al., 2011; Zhang et al., 2009). TDP-43 pathology was also observed in pathological brain regions of Frontotemporal Lobar Degeneration (FTLD) and Alzheimer's disease (Wilson et al., 2011) in which RNA editing was efficient, suggesting that there were several different causes for TDP-43 pathology. TDP-43 pathology consists of a combination of molecular abnormalities including absence from the nucleus, where it normally resides, mislocalization to abnormal cytoplasmic inclusions and abnormal fragmentation and hyperphosphorylation (Arai et al., 2006; Chen-Plotkin et al., 2010; Hasegawa et al., 2008; Neumann et al., 2006).

TDP-43 pathology is believed to be initiated from the formation of small aggregates that are generated by fragmentation of TDP-43 in the cytoplasm, which serve as seeds for large inclusions that increase in size with sequestration of full-length and fragments of TDP-43 (Chen-Plotkin et al., 2010). Although protease-dependent cleavage of TDP-43 is likely a trigger for TDP-43 pathology, neither the proteases involved nor the mechanism of protease activation are known. TDP-43 pathology is rarely, if ever, observed in the motor neurons of patients who have *SOD1*-associated ALS or in *SOD1* Tg animals (Mackenzie et al., 2007; Robertson et al., 2007; Tan et al., 2007). Moreover, inefficient RNA editing at the GluA2 Q/R site in motor neurons of sporadic ALS does not occur in *SOD1* Tg rats (Aizawa et al., 2010; Kawahara et al., 2006). The difference, in light of TDP-43 processing and ADAR2 regulation, between these two ALS model lines suggests a mechanistic difference between *SOD1*-associated ALS and sporadic ALS. Notably, disease-specific abnormalities of both ADAR2 underactivity and TDP-43 pathology were concomitantly observed in the same motor neurons of sporadic ALS patients, suggesting a molecular link between these two molecular abnormalities (Aizawa et al., 2010). Furthermore, these two molecular abnormalities in motor neurons were observed not only in sporadic ALS patients but also in elderly humans and mice (Geser et al., 2010; Hideyama et al., 2012a), providing evidence that there is an intimate molecular linkage between both (Fig. 2).

Experiments using various lines of cultured cells demonstrated that none of TDP-43 overexpression, TDP-43 knockdown, TDP-43 C-terminal fragments or TDP-43 mutations, changed the expression levels of ADAR2 (Yamashita et al., 2012b). These results suggest that the abnormal processing of TDP-43 is not an upstream event of inefficient GluA2 Q/R site RNA editing in the motor neurons of sporadic ALS patients.

The downregulation of ADAR2 in motor neurons of sporadic ALS patients occurred before RNA editing at the GluA2 Q/R site was inefficient, and TDP-43 pathology was generated only in motor neurons that have very low ADAR2 expression (Hideyama et al., 2012b). ADAR2-lacking motor neurons in AR2 and AR2H mice underwent death via a Ca^{2+}-permeable AMPA receptor-mediated mechanism (Hideyama et al., 2010; Hideyama and Kwak, 2011), and exhibited loss of TDP-43 from the nucleus and TDP-43-containing abnormal aggregates in the cytoplasm (Figs. 1 and 3) (Yamashita et al., 2012a). *In vitro* calpain assay demonstrated that TDP-43 was specifically cleaved by calpains. Cleavage of TDP-43 was inhibited by endogenous and exogenous calpain inhibitors both *in vivo* and *in vitro* and when the AR2 mice were engineered to express Ca^{2+}-impermeable AMPA receptors with GluA2R in the absence of ADAR2 by crossing with GluR-$B^{R/R}$

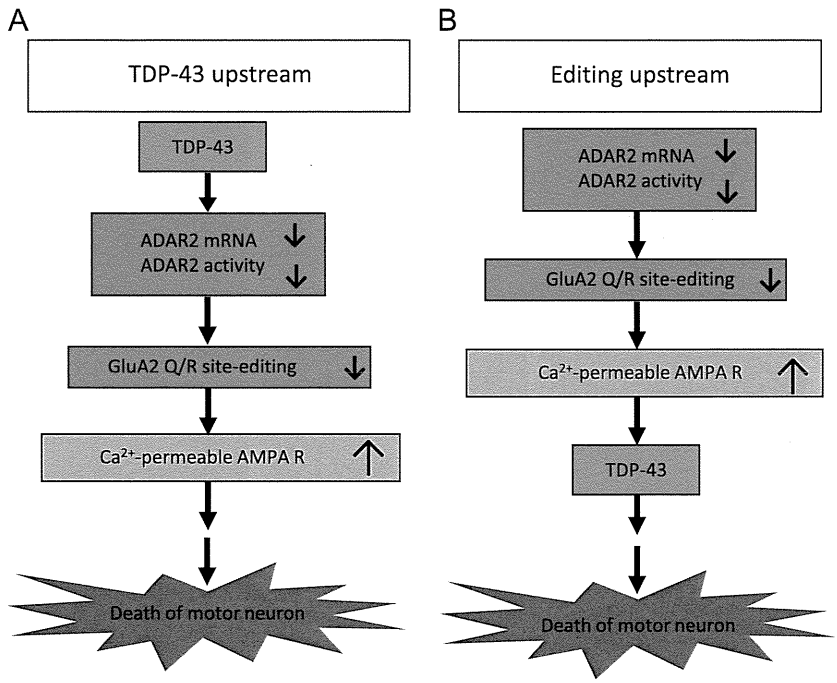

Fig. 2 – The cascades of RNA editing at the GluA2 Q/R site and abnormal TDP-43 processing: (A) illustration of the hypothesis that TDP-43 processing abnormality induces deficient ADAR2. (B) Illustration of the hypothesis that ADAR2 underactivity influences the generation of TDP-43 pathology.

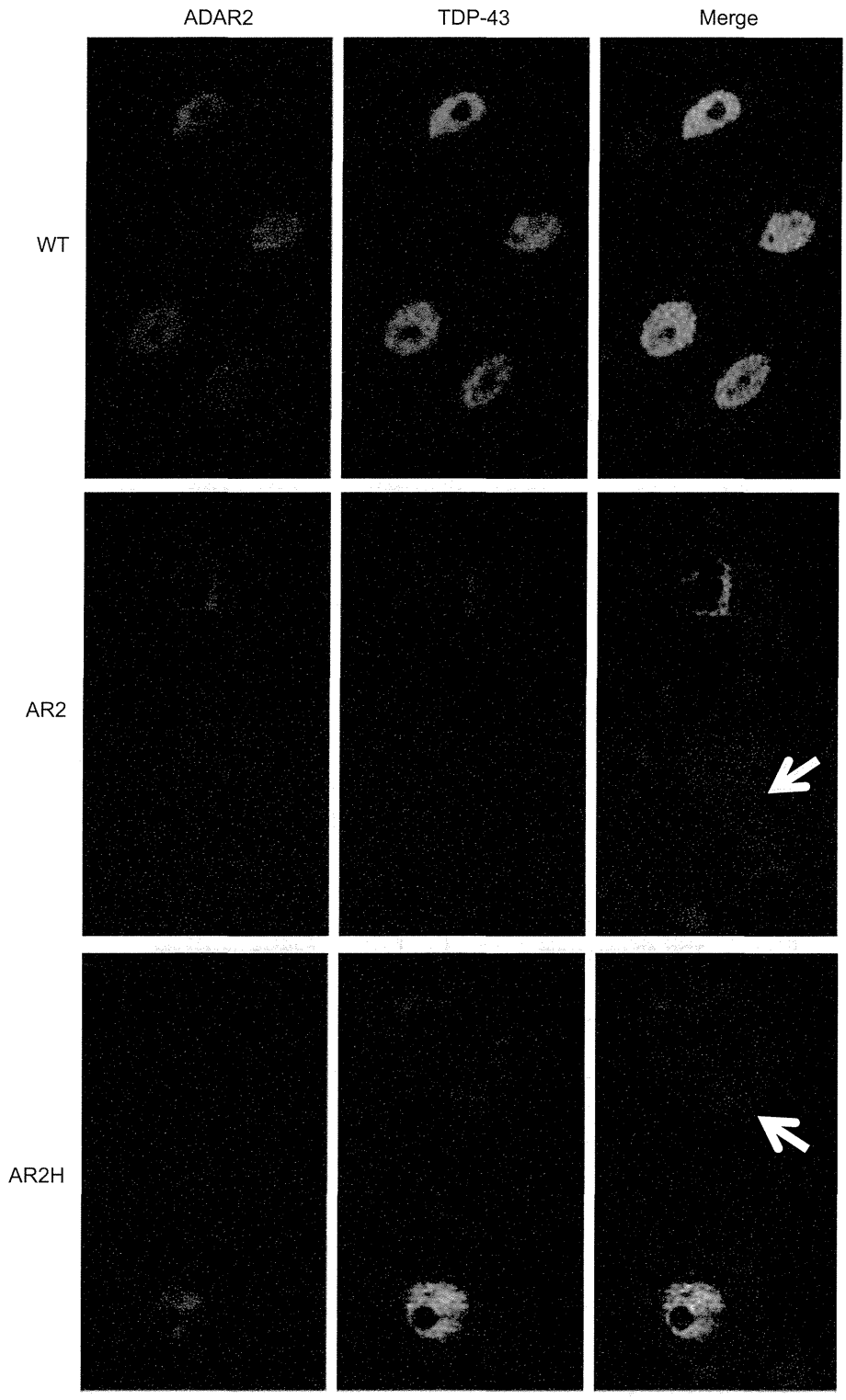

Fig. 3 – TDP-43 pathology and ADAR2 in spinal motor neurons (AHCs) (AR2 and AR2H). Immunofluorescence assays revealed that ADAR2 (red) and TDP-43 (green) both localize to the nucleus in control AHCs.TDP-43 immunoreactivity was absent in AHCs that lack ADAR2 in AR2 mice (arrow). AHCs with low immunoreactivity for ADAR2 showed TDP-43 immunoreactivity in the cytoplasm and TDP-43-positive cytoplasmic aggregates in heterozygous AR2 mice (AR2H) (arrow). TOPRO-3 is a cellular maker (blue).

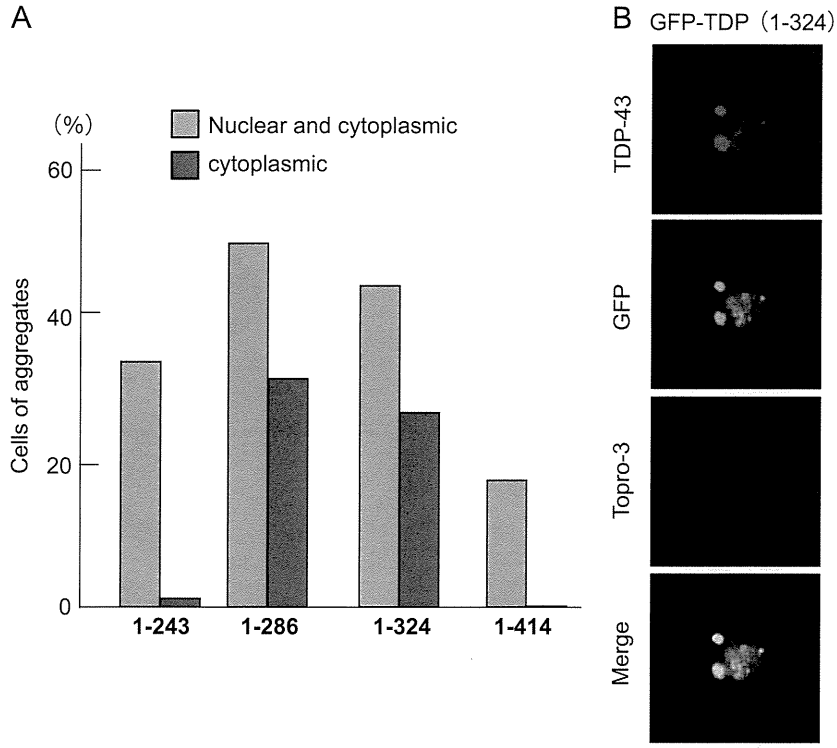

Fig. 4 – Aggregation of calpain-dependent TDP-43 N-terminal fragments: (A) the proportion of cells that have aggregates among those exhibiting GFP signals was calculated. The larger calpain-dependent TDP-43 fragments (1–286 and 1–324) induced cytoplasmic aggregations in a larger number of cells than the full-length TDP-43 (1-414) or the small calpain-dependent TDP-43 fragment (1–243). (B) Examples of cells 72 h after transfection with the GFP-TDP-43 fragment (1–324). TDP-43-positive aggregates formed in the nucleus and cytoplasm of culture cells transfected with the GFP-TDP-43 fragment (1–324).

mice (Hideyama et al., 2010; Kask et al., 1998). Conversely, both TDP-43 cleavage and mislocalization in the neurons were exaggerated in calpastatin knockout mice. These results indicated that the fragmentation and abnormal localization of TDP-43 observed in AR2 and AR2H mice were dependent on the activation of calpain through Ca^{2+}-permeable AMPA receptors (Yamashita et al., 2012a).

The Ca^{2+}-dependent serine protease calpain cleaved TDP-43 at several positions in the C-terminal region and the resulting N-terminal fragments were prone to aggregation (Fig. 4) (Yamashita et al., 2012a). In the brains and spinal cords of ALS patients, calpain is more active compared to normal control subjects and calpain-dependent TDP-43 fragments were demonstrated in the lysates and sarkosyl-insoluble fraction, suggesting that the calpain-dependent cleavage of TDP-43 may be involved in the pathogenesis of TDP-43 pathology of ALS motor neurons the same as observed in AR2 mouse motor neurons (Yamashita et al., 2012a).

There were many reports indicating that the TDP-43 cleavage was caused by caspase-3 (Dormann et al., 2009; Igaz et al., 2009; Zhang et al., 2007) and loss of function of the progranulin has been suggested to lead to caspase-3 activation. The caspase-3-dependent proteolysis of the TDP-43 generated C-terminal fragments (CTFs) but researchers demonstrated the presence of TDP-43 CTFs that were generated by caspase-dependent and -independent cleavage (Herskowitz et al., 2012; Nishimoto et al., 2009; Nonaka et al., 2009) and fragments consistent with those generated by cleavage with both calpain and caspase-3 was demonstrated in sporadic FTLD-ALS brain and spinal cord extracts (Yamashita et al., 2012a). These observations suggest that caspase-3-dependent cleavage of TDP-43 may participate in TDP-43 pathology by cleaving the full-length and calpain-dependent fragments of TDP-43 into aggregation-prone fragments. However, caspase-3 cleaved TDP-43 far less effectively than calpain (Yamashita et al., 2012a) and caspase-3 was activated after the activation of calpain in the brains of excitotoxic model animals (Takano et al., 2005), suggesting the minor participation of caspases in TDP-43 compared to calpains.

Taken together, these results indicate that the calpain-dependent cleavage of TDP-43 plays a crucial role in ALS pathology (Fig. 5), although the link between the formation of TDP-43 aggregation and cell death is unknown.

5. *TARDBP*-associated ALS and Calpain

TDP-43 pathology appears in the motor neurons of patients with ALS associated with mutations in the *TARDBP* gene as well as sporadic ALS patients who express wild-type TDP-43 (Arai et al., 2006; Chen-Plotkin et al., 2010; Hasegawa et al., 2008; Lagier-Tourenne et al., 2010; Neumann et al., 2006). Although an increased vulnerability of cultured cells expressing mutant TDP-43 compared to those expressing wild-

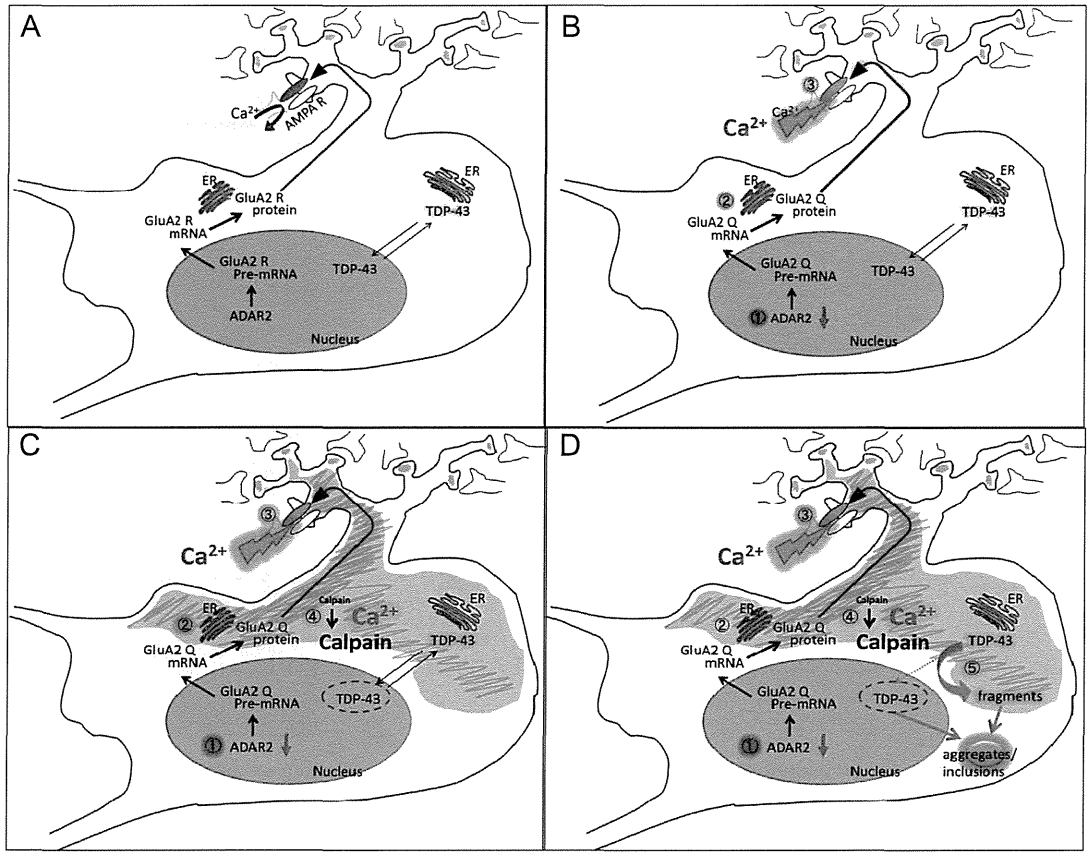

Fig. 5 – Schematic illustration of the molecular mechanism underlying TDP-43 pathology in sporadic ALS motor neurons: (A) Normal neurons. (B) Motor neurons of sporadic ALS patients: downregulation of ADAR2→failure of RNA editing at the Q/R site of GluA2 pre-mRNA→expression of calcium-permeable AMPA receptors (AMPA R) at the synaptic spines. (C) An increase of cytoplasmic calcium concentration. Activation of calpain. (D) Cleavage of TDP-43 by activated calpain→aggregation of TDP-43 fragments→ sequestration of TDP-43 that shuttles between the nucleus and the cytoplasm into the aggregates, resulting in the large inclusions.

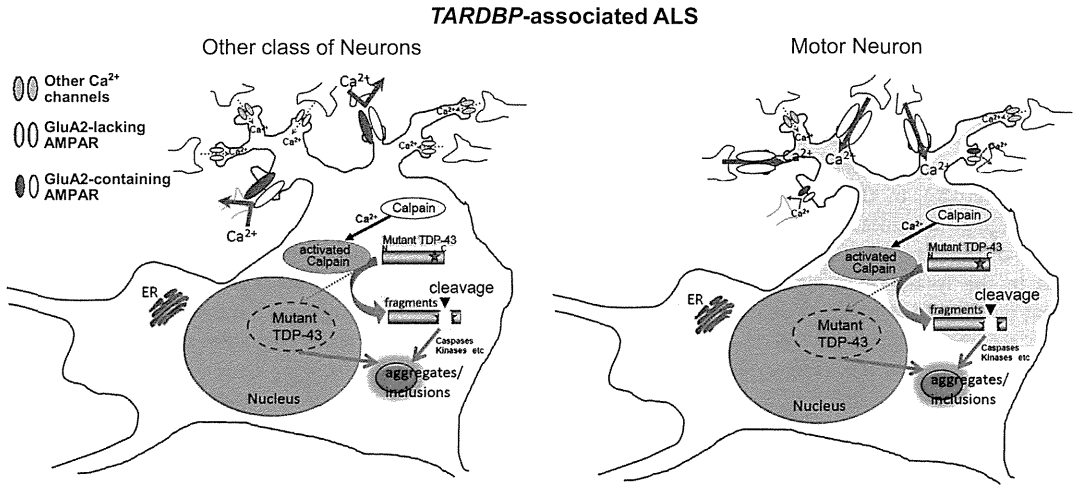

Fig. 6 – Schematic illustration of the molecular mechanism underlying *TARDBP*-ALS motor neuron and other class of neurons. The expression of ADAR2 is normal, and Q/R site-edited GluA2 is expressed with normal activation of calpain in *TARDBP*-ALS. In *TARDBP*-ALS motor neurons, calpain activity is higher than in other classes of neurons presumably due to the higher expression level of GluA2-lacking Ca^{2+}-permeable AMPAR. The increased vulnerability of mutant TDP-43 to calpain-mediated cleavage in motor neurons with physiologically high calpain activity generates more abundant highly aggregation-prone fragments in the motor neurons than in other classes of neurons of *TARDBP*-ALS patients.

type TDP-43 has been demonstrated (Gitcho et al., 2008; Sreedharan et al., 2008), molecular mechanisms whereby mutant and wild-type TDP-43 exhibit similar pathology have not been elucidated. Recent finding that ALS-linked mutant TDP-43 (A315T, M337V) was more effectively cleaved by calpains than wild-type TDP-43 suggested that increased liability to calpain-dependent cleavage was involved in the TDP-43 pathology observed in the motor neurons of *TARDBP*-ALS patients. In addition, the increased susceptibility of mutant TDP-43 to calpain cleavage enables to explain the finding that patients who have mutations in the *TARDBP* gene exhibit an ALS phenotype but not, or at least very infrequently, a frontotemporal dementia (FTD) phenotype (Chen-Plotkin et al., 2010). Ca^{2+} influx through the AMPA receptors is known to be greater in the spinal motor neurons than in the dorsal horn neurons in a primary culture of spinal cord neurons (Carriedo et al., 1996), and calpain activity in the spinal motor neurons was greater than in other neurons, such as cortical and dorsal horn neuron of autopsied human subjects free from neurological diseases (Yamashita et al., 2012a). Spinal motor neurons express relatively low levels of GluA2 compared to other classes of neurons in humans and rodents (Carriedo et al., 1996; Kawahara et al., 2003; Sun et al., 2005), indicating that more abundant AMPA receptors lacking GluA2 resulted in higher Ca^{2+} influx through AMPA receptors and calpain activity in motor neurons than in other class of neurons (Fig. 6). These lines of evidence suggest that a greater amount of TDP-43 fragments would be generated in the motor neurons in which Ca^{2+}-permeable AMPA receptors lacking GluA2 are abundantly expressed, and the motor neuron-prone generation of TDP-43 pathology results in ALS phenotype in *TARDBP* patients (Chen-Plotkin et al., 2010; Lagier-Tourenne et al., 2010). Therefore, although the role of calpain is critical in TDP-43 pathology, different mechanisms may enhance calpain-dependent TDP-43 cleavage between sporadic ALS and *TARDBP*-ALS. In sporadic ALS, activation of calpain by increased Ca^{2+} influx through the upregulation of Ca^{2+}-permeable AMPA receptors containing GluA2Q enhanced TDP-43 cleavage, whereas the increased vulnerability of mutant TDP-43 to calpain-mediated cleavage generates abnormal TDP-43 fragments in *TARDBP*-ALS motor neurons where calpain activity is higher than in other classes of neurons presumably due to the higher expression level of GluA2-lacking Ca^{2+}-permeable AMPA receptors.

In motor neurons of both sporadic ALS and *TARDBP*-associated ALS, highly aggregation-prone calpain-dependent TDP-43 fragments generated cytoplasmic inclusions to which nucleocytoplasm shuttling TDP-43 was sequestered and disappeared from the nucleus (Figs. 5 and 6) (Yamashita et al., 2012a). These results suggest that the same pathology would be generated from different mechanisms and that we should be prudent to assess the pathological hallmark as a disease hallmark.

6. TDP-43 pathology in other neurological diseases

TDP-43 pathology is observed not only in ALS motor neurons and FTLD-TDP cortical neurons but also in pathological brain regions of various other neurological diseases, including Alzheimer's disease (Wilson et al., 2011) and traumatic brain injury (McKee et al., 2010), as well as in the CNS of animals exposed to various adverse conditions, including sciatic axotomies (Moisse et al., 2009) and brain ischemia (Kanazawa et al., 2011). Because Ca^{2+} dysregulation and calpain activation have been reported in various diseases (Lopatniuk and Witkowski, 2011), calpain activated via various abnormal Ca^{2+} signaling pathways could play important roles for TDP-43 pathology. In fact, age-associated calpain activation may be involved in the mechanism underlying mislocalization of TDP-43 from the nucleus to the cytoplasm that is observed in the cortical neurons of normal elderly people (Geser et al., 2010) and motor neurons of aged mice (Hideyama et al., 2012a). Scrutiny of the roles of various pathways causing Ca^{2+} dysregulation in the pathological conditions in TDP-43 may improve our knowledge about the mechanism generating TDP-43 pathology in various neurological diseases other than ALS.

7. Conclusion and future directions

In this review, we summarized the evidence indicating the role of inefficient RNA editing in the pathogenesis of sporadic ALS. These molecular abnormalities cause death of motor neurons and TDP-43 pathology in the motor neurons of the conditional ADAR2 knockout mouse, a mechanistic model of sporadic ALS. However, we still do not know how the mislocalization of TDP-43 leads motor neurons to death or whether the mislocalization of TDP-43 occurs in the death cascade or merely an associated phenomenon observed downstream of ADAR2 downregulation.

Another unresolved question is why ADAR2 is downregulated in ALS motor neurons. Recent studies on dysfunction of some ALS associated genes seem to provide us a clue for the mechanism. ALS-linked genes encode proteins involved in RNA processing, and using iPS cells, fibroblasts and brains from patients carrying expansion of GGGGCC repeat in C9orf72 gene, an ALS-linked gene, several reports showed formation of abnormal RNA foci in which some RNA-binding proteins, including ADARB2 (or ADAR3) protein, a member of the RNA editing enzyme family, were demonstrated (Donnelly et al., 2013; Gendron et al., 2013; Lagier-Tourenne et al., 2013; Sareen et al., 2013; Zu et al., 2013). Furthermore, nuclear-enriched abundant transcript 1_2 (NEAT1_2), a long non-coding RNA, was demonstrated to bind to TDP-43 and FUS/TLS (products of an ALS-linked gene) in the spinal motor neurons of ALS patients (Nishimoto et al., 2013). These lines of evidence suggest that abnormal RNA-associated foci generated by dysfunction of ALS-associated genes may act as a scaffold of RNAs and RNA binding proteins in the nuclei of ALS motor neurons, thereby modulating the gene expression that is critical for neuronal survival (Donnelly et al., 2013; Kwak and Kawahara, 2005). Because ADAR2 downregulation is one death-causing molecular abnormalities demonstrated in ALS motor neurons, scrutiny for the effects of sequestration of gene-regulatory molecules on ADAR2 gene expression may provide us a clue for the mechanism underlying the ADAR2 downregulation and ALS pathogenesis.